

UNCLASSIFIED

AD 4 2 2 3 8 7

DEFENSE DOCUMENTATION CENTER

FOR

SCIENTIFIC AND TECHNICAL INFORMATION

CAMERON STATION, ALEXANDRIA, VIRGINIA



UNCLASSIFIED

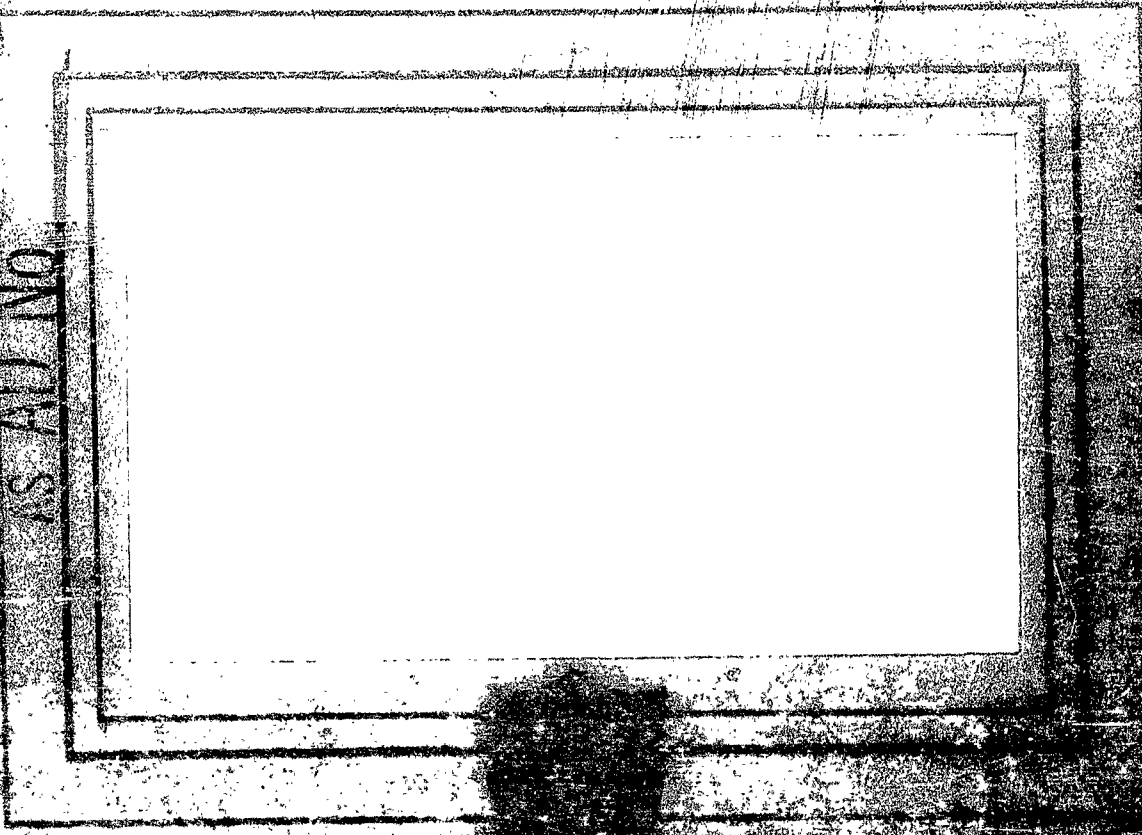
DISCLAIMER NOTICE

**THIS DOCUMENT IS BEST QUALITY
PRACTICABLE. THE COPY FURNISHED
TO DTIC CONTAINED A SIGNIFICANT
NUMBER OF PAGES WHICH DO NOT
REPRODUCE LEGIBLY.**

NOTICE: When government or other drawings, specifications or other data are used for any purpose other than in connection with a definitely related government procurement operation, the U. S. Government thereby incurs no responsibility, nor any obligation whatsoever; and the fact that the Government may have formulated, furnished, or in any way supplied the said drawings, specifications, or other data is not to be regarded by implication or otherwise as in any manner licensing the holder or any other person or corporation, or conveying any rights or permission to manufacture, use or sell any patented invention that may in any way be related thereto.

CATALOGUED BY DDC 12238

AS AD INQ



DDC
12238
100-5-100
100-5-100
100-5-100

PRINCETON UNIVERSITY
DEPARTMENT OF AERONAUTICAL ENGINEERING

DEPARTMENT OF THE NAVY
OFFICE OF NAVAL RESEARCH
POWER BRANCH
(ADVANCED RESEARCH PROJECTS AGENCY)

Contract Nonr 1858(32)
Project No. NR 098-201 - Amend. 4
(ARPA Order No. 23-63 - Amendment 21)

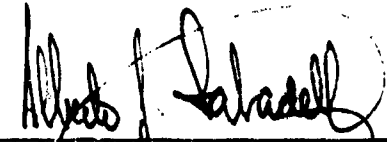
THE MEASUREMENT OF THE TEMPERATURE
PROFILES OF BURNING SOLID PROPELLANTS
BY MICROTHERMOCOUPLES

Technical Report

1 January 1962 to 30 September 1963

Aeronautical Engineering Report No. 664

Prepared by:


Alberto J. Sabadell
Research Assistant

and:


Joseph Wenograd
Research Associate

Approved by:


Martin Summerfield
Principal Investigator

Reproduction, translation, publication, use and disposal in whole or in part by or for the United States Government is permitted.

23 September 1963

Guggenheim Laboratories for the Aerospace Propulsion Sciences
Department of Aeronautical Engineering
PRINCETON UNIVERSITY
Princeton, New Jersey

The contents of this report have been submitted in partial fulfillment of the requirements for the degree of Master of Science in Engineering from Princeton University, 1963.

ACKNOWLEDGMENTS

The author would like to express his gratitude to all those persons and organizations who through their advice, assistance or encouragement have supported this thesis.

Financial support for this work was received from Princeton University, NASA, ONR-ARPA, and the Ministry of Defense of Argentina.

Credit is deserved by the Jet Propulsion Group of the Aeronautical Engineering Department of Princeton University. The author is especially grateful to the entire Solid Propellant Group for their interest and advice.

The author wishes to acknowledge the constant assistance received from Dr. Joseph Wenograd toward the realization of this program.

Finally, it has been the privilege of the author to work under the guidance of Professor Martin Summerfield, without whose personal interest this research could not be possible. For all that the author expresses his sincere appreciation.

ABSTRACT

A knowledge of the temperature which prevails at the surface of a burning solid propellant and the functional dependence of this temperature on various parameters are important factors contributing to a basic understanding of the combustion mechanism. In this research, attempts have been made to obtain this information through studies of the temperature profile in the solid pre-heat zone, and the gaseous combustion zone of burning solid propellants. These temperature profiles have been obtained by allowing solid propellant strands to burn past very fine, embedded thermocouples.

Techniques have been developed for the routine fabrication and handling of micro-thermocouples made from platinum-platinum 10% rhodium Wollaston wire with .0003 inch or finer diameter. Thermocouples with bead sizes no larger than 15 microns are cast into composite propellants or glued into double base propellants. The casting of these thermocouples into composite propellants, primarily a PBAA binder containing 70% fine (9 μ) ammonium perchlorate, has been accomplished with a thermocouple recovery rate of approximately 65%.

With the propellant strand burning in cigarette fashion, the thermal wave passes over the thermocouple. The voltage vs. time trace thus obtained permits the determination of the temperature distribution in the combustion wave.

Analysis of this curve by means of the steady-state energy equation with appropriate assumptions, gives a method for determining the surface temperature of the propellant as had been developed by Klein, et al. (17).

Temperature time records for composite and double base propellants have been obtained under a variety of conditions. In general, the records for double base propellants are much smoother than the corresponding composite records. This behavior is quite reproducible and it must be concluded that the irregularities in the composite records are caused by the heterogeneous nature of the conduction path between the thermocouple and the burning surface. Surface temperatures in the range 550-650° C. for combustion between atmospheric and 200 psig have been observed for the composite propellants studied. Thermal conductivities were found between $5.5 - 12.5 \times 10^{-4}$ cal/cm sec °K. The range of uncertainty could be due either to the composite nature of the propellant or to microscopic deviations from the average burning rate. A double base propellant has been found to burn with a surface temperature of about 300° C. with similar variations in thermal conductivity.

TABLE OF CONTENTS

	Page
TITLE PAGE	i
ACKNOWLEDGMENTS	ii
ABSTRACT	iii
TABLE OF CONTENTS	v
LIST OF TABLES	vii
LIST OF FIGURES	viii
CHAPTER I. INTRODUCTION AND OBJECTIVES OF RESEARCH	1
A. General	1
B. Description of Burning Process	2
C. Theories of Combustion	3
D. Purpose	9
CHAPTER II. REVIEW OF LITERATURE ON THERMAL STRUCTURE STUDIES	10
A. Thermal Structure Measurements in Double Base Propellants	10
B. Thermal Distribution in Liquid Nitrate Ester Strands	13
C. Thermal Wave Structure in Solid Composite Propellants	15
CHAPTER III. APPLICATION OF THERMOCOUPLE TECHNIQUE	17
A. Experimental Program	17
1. Thermocouple Fabrication	17
2. Propellant	18
3. Embedding of Thermocouples	19
4. Experimental Apparatus	20
5. Strand Burner	21
6. Double Base Experiments	23
B. Determination of Surface Temperature	24
C. Data Reduction	26
D. Measurement Limitations	27
1. Remarks on Thermocouple Technique	27
2. Surface Temperature	28
3. Coefficient of Thermal Conductivity	29
E. Type of Results Expected	29
CHAPTER IV. RESULTS	31
A. Surface Temperature	31
B. Coefficient of Thermal Conductivity	32
C. Comparision of Double Base and Composite Propellant Temperature Profiles	33
D. Gas Temperature	34

TABLE OF CONTENTS - contd.

	Page
CHAPTER V. DISCUSSIONS AND CONCLUSIONS	35
A. Differences Between Double Base and Composite Propellants	35
1. Physical Interpretation	35
2. Analysis	36
B. Surface Temperature	40
C. Coefficient of Thermal Conductivity	41
CHAPTER VI. RECOMMENDATIONS	43
Appendix A: Secondary Thermoelectric Effect on Wollaston Wires	A-1
B: Thermocouple Production Technique	B-1
C: Propellant Processing	C-1
D: Embedding of Thermocouples	D-1
E: Conductance Probe as an Auxiliary Tool for Surface Temperature	E-1
F: Solution of Heat Balance Equation [III-2]	F-1
G: Commercial Equipment and Materials	G-1

REFERENCES

TABLES

FIGURES

LIST OF TABLES

- I. Description of propellant compositions.
- II. Calculation performed on test shown in Figure 12.
- III. Average values of T_s and λ for different compositions tested.
- IV. Values of T_s and λ for particular tests shown in Figures 14A to 20A.

LIST OF FIGURES

1. Apparatus and tools employed for fabrication of microthermocouples
2. Burning rate vs. pressure for propellant compositions studied
3. Propellant casting apparatus
4. Sequence showing technique for embedding thermocouple in strand
5. Electronic recording instrumentation for thermocouple traverses
6. Schematic representation of instrumental setup for thermocouple traverses
7. Strand ready for test in chimney strand burner
8. Control panel for strand burning rate apparatus
9. Strand burner
10. Strand holder prepared for a test
11. Model of one-dimensional steady-state burning
12. Voltage-time record showing method of obtaining data
13. $\log (T - T_o)$ versus time corresponding to test shown in Figure 12
- 14A. Voltage-time record for PBAA 70F, burning at 30 psig
- 14B. $\log (T - T_o)$ vs. time corresponding to test shown in Figure 14A.
- 15A. Voltage-time record for PBAA 70F, burning at 100 psig
- 15B. $\log (T - T_o)$ vs. time corresponding to test shown in Figure 15A.
- 16A. Voltage-time record for PBAA 70F, burning at 150 psig
- 16B. $\log (T - T_o)$ vs. time corresponding to test shown in Figure 16A.
- 17A. Voltage-time record for PBAA 70F, burning at 30 psig, thermocouple of 2.5 μ diameter wires
- 17B. $\log (T - T_o)$ vs. time corresponding to test shown in Figure 17A.
- 18A. Voltage-time record for PBAA 75 BM, burning at 30 psig
- 18B. $\log (T - T_o)$ vs. time corresponding to test shown in Figure 18A.

LIST OF FIGURES - contd.

- 19A. Voltage-time record for double base propellant burning at 50 psig
- 19B. $\log (T - T_o)$ vs. time corresponding to test shown in Figure 19A.
- 20A. Voltage-time record for double base propellant burning at 150 psig
- 20B. $\log (T - T_o)$ versus time corresponding to test shown in Figure 20A.
- 21. $\log \Theta$ versus time for a double base temperature traverse
- 22. $\log \Theta$ versus time for a PBAA 70F temperature traverse
- 23. Coefficient of thermal conductivity versus burning rate for different propellants tested
- 24. X-ray picture of strand with thermocouple and fuse wire embedded

CHAPTER I

INTRODUCTION AND OBJECTIVES OF RESEARCH

A. General

The use of solid rocket propellants in modern aerospace technology is highly developed. The state of the art is such that the engineering of solid propellant systems has been accomplished with considerable rapidity. In contrast, the scientific knowledge of the complicated physico-chemical processes involved in the mechanism of combustion of solid propellant is far from complete, due in part to a lack of experimental data. The present work is part of the efforts conducted at Princeton University aimed at the phenomenological description of this process.

Modern solid propellants are divided into two classes according to their composition and physical structure, double base and composite propellants. Double base propellants consist mainly of nitrocellulose and nitroglycerine, and small amounts of other additives as stabilizers, coolants, burning rate modifiers, etc. Their compositions derive from the very well-known gun powders used for many years. The end product is a rigid colloid of microscopically homogeneous structure.

Composite propellants consist of finely divided crystalline oxidizer dispersed in a solid organic matrix. There are a great variety of compositions according to the oxidizer and binder used. The oxidizer can be inorganic nitrates or perchlorates, of which ammonium perchlorate is the most widely used. Matrix materials

can be almost any plastic, resinous or elastomeric binder. The common characteristic of all these mixtures is the heterogeneous structure of the end product.

Despite their gross differences, both types of composition have evident similarities in their burning behavior. This generalization shows well in the dependence of burning rate on pressure for both classes of propellant as expressed by the law of Vieille

$$r = b p^n$$

[I-1]

where b and n are constants characteristic of the particular mixture under study.

B. Description of Burning Process

A general description of the different steps involved in the combustion process could be the following. In the solid, due to the low thermal conductivity, the propellant at a short distance below the surface is unaffected. As the burning surface approaches, the propellant temperature rises due to heat conduction, and possibly chemical reaction as occurs, for example, in the foam zone of double base compositions. As the propellant temperature reaches the burning surface value, the solid components volatilize; these volatile products then react in the gas phase giving the high propellant flame temperature.

In order to satisfy this description, it is necessary that somewhere a phase-change occurs,

transforming the solid components into gaseous products. At this solid surface the gasification may take place through an equilibrium process or a chemical kinetically-controlled phenomenon. In either case, the temperature of that surface is a fundamental parameter in the description of the burning mechanism. The state of that surface is supposed to be smooth for double base propellants, and consequently the surface temperature may have a well-defined value. But for composite propellants, due to their heterogeneous nature, the surface consists of a distribution of oxidizer crystals and fuel pockets, each of which might have a different surface temperature. Thus, the surface temperature may vary from point to point.

C. Theories of Combustion

A review of the theories of solid propellant combustion has been done elsewhere. In Geckler (1) and Sutherland (2), a review on double base combustion is given. Schultz, Green and Penner (3) survey the theories for composite propellant combustion.

Wilfong, Penner and Daniels (4) have proposed a simple description for the thermal decomposition of a double base propellant. They assume that the rate controlling reaction occurs in a monomolecular surface layer and is governed by an Arrhenius type equation:

$$r = B \exp\left(-\frac{E_s}{RT_s}\right) \quad [I-2]$$

where B is the frequency factor, E_s is the activation

energy, R is the molar gas constant and T_s is the surface temperature. B and E_s are assumed to be constants independent of temperature. This proposition then gives the dependence of burning rate upon T_s .

More elaborated theories have been postulated. Each of them is based on the assumption of a feedback of energy from the gas phase reaction to the solid surface. The burning rate is then related to that feedback of heat. For double base propellants the results of some experiments on the physical structure of the flame (5) has led to a model of combustion process that may account for the burning rates experimentally encountered. The analysis of Rice and Ginell (6), and Parr and Crawford (7), both make the basic assumption that the different steps of the combustion process are simple one-dimensional reaction zones to which well-known, premixed, laminar flame theories can be applied.

The application of these simple theories to the complex burning mechanism of the heterogeneous composite propellant does not seem to be valid. The three-dimensional effects of the separate gasification of the fuel and oxidizer, the mutual diffusion of one into the other with partial reaction, and the final chemical reaction of the premixed gases, should be taken into account in the development of a complete theory.

Rice (8) was the first to point out the fundamental difference between the combustion of double base and composite propellants. He proposed that the vaporization of fuel and oxidizer takes place independently in a smooth surface giving gaseous streams of fuel and oxidizer, and then burn as a typical laminar-diffusion

flame in form of axisymmetric jets. The surface temperature is not important, but the time required for mixing by diffusion is then of dominant importance.

Nachbar (9), based on a model described by Schultz, Green and Penner (3), postulates an idealized sandwich model composed of alternating slabs of fuel and oxidizer. An expression for the burning rate of this geometry is obtained as a function of the surface temperature of the oxidizer particle. This solution does not show the variation of burning rate with pressure.

Chaiken (10), based on the "two-temperature" model described by Schultz, Green and Penner (3), postulates that the surface decomposition is the controlling mechanism. Looking on a microscopic scale the two constituents gasify independently from the surface, following a pyrolysis law of the Arrhenius type. But since in steady-state burning the mean regression rate of the propellant must be equal to the mean regression rate of the fuel and the oxidizer, it follows that

$$\dot{r}_p = B_{s,o} \exp\left(-\frac{E_{s,o}}{RT_{s,o}}\right) = B_{s,f} \exp\left(-\frac{E_{s,f}}{RT_{s,f}}\right) \quad [\text{I-3}]$$

where \dot{r}_p is the regression rate of the propellant surface, B_s are the frequency factors, E_s are the activation energies and T_s are the temperature values at the surface for oxidizer (o) and fuel (f).

Now, since the constants B_s and E_s are different for each component it follows that the mean

surface temperature of oxidizer and fuel during burning are necessarily different, and correspondingly they will have unequal mean depths, one component protruding over the other. With this model Chaiken postulates his "thermal layer" theory based in the following combustion process steps. The oxidizer crystals gasify by an endothermic reaction, then the oxidizer pyrolysis products react exothermically establishing a flame. The fuel pyrolyzes into this oxidizer flame and oxidation-reduction gas-phase final reactions take place between fuel and oxidizer pyrolysis products. The last step is supposed to occur far away from the surface and only the oxidizer pyrolysis products reaction affects the surface, controlling then the burning rate. This theory has been developed for ammonium nitrate propellants. If reasonable estimates of the physico-chemical properties are made, this theory is able to correlate the experimental and estimated values of burning rates for this class of propellant.

Levy and Friedman (11), based on results of experiments on the decomposition of pure ammonium perchlorate, postulate like Chaiken, that the linear burning rate of ammonium perchlorate propellants is primarily determined by the oxidizer decomposition. This theory is probably applicable at pressures higher than 1000 psi, but below that pressure it can not explain the effects of particle size, oxidizer-fuel ratio and burning rate plateaus.

In contrast with the preceding theories, Summerfield postulated the "Granular Diffusion Flame Theory" (12), which predicts the effects of pressure, particle size and fuel-oxidant ratio. The correlation

of the theory with experimental results has been done through extensive research work performed by different co-workers. Sutherland (2) revealed the structure of the flame zone. Webb (13) and Taback (14) investigated the experimental dependence of burning rate on pressure for different fuel-oxidant ratios of an unmodified composite propellant, and also with addition of catalyst and other control factors. Bastress (15) analyzed the effect of oxidizer particle size upon burning rate.

The granular diffusion flame takes its name from the assumption that the fuel and oxidizer vaporize into gaseous pockets or granules. Since there is more oxidant atmosphere than fuel gas, the pockets are probably constituted of gaseous fuel surrounded by oxidant gas. The surface is assumed to be dry, and there is no chemical reaction in the solid phase. On a microscopic scale it is a three-dimensional diffusional process, followed by chemical reaction of the homogeneous premixed gaseous phase.

The exposed surface decomposes due to heat fed back from the hot flame. Radiation and molecular diffusion are neglected. In these conditions the theory establishes the heat balance equation at the surface.

The theory accepts the "two temperature" postulate (3) already described, but for simplicity T_s is replaced by the average of the two temperatures. Furthermore, T_s is assumed independent of pressure, which is true if the activation energy is large compared with RT_s in the Arrhenius equation. If this was not the case, an Arrhenius type equation should be added to the analysis and solved together with the energy equation to account for the dependence of τ and T_s on pressure.

To obtain the burning rate from the energy equation it is necessary to have an expression for the flame thickness L , that appears in the heat balance equation. That is done by considering two limiting cases.

First, at high pressure, a thin reaction zone occurs and the diffusional mechanism is the limiting factor. This allows the calculation of a "diffusional flame thickness," L_1 .

The second limiting case is at low pressures where chemical reaction is the limiting factor, and interdiffusion occurs before appreciable reaction takes place. The combustion proceeds as a premixed gaseous flame, where a second order reaction is taking place. From this a "chemical flame thickness" is obtained, L_2 .

The flame thickness for intermediate pressure is described, following Powell (16), by the addition of L_1 and L_2 with small coefficients, of order unity.

By appropriate manipulation of the equations deduced in the preceding description, the theory establishes the dependence of burning rate on pressure with the following equation:

$$\frac{1}{r} = \frac{a}{p} + \frac{b}{p^{1/2}} \quad [I-4]$$

where a is a chemical reaction parameter showing the influence of the flame temperature. And b is a diffusion time parameter that shows the effect of particle size. The effect of T_s appears in both coefficients.

D. Purpose

All the theories hitherto described regard the surface gasification as an essential process. The state of the surface and especially its temperature is then of fundamental importance in determining the surface regression rate and the possibility of a phenomenological correlation with the experimental results.

Furthermore, an analysis of the temperature profile should be able to point out the differences in physical structure of the several propellants under study, especially between microscopically homogeneous and heterogeneous propellants.

In consequence, the present work was aimed at obtaining the thermal wave structure in the combustion of a solid composite propellant. Special attention was directed to the subsurface temperature history so as to identify the surface temperature.

To accomplish this end the following steps were necessary. A technique for production of micro-thermocouples of 7.5 and 2.5 μ wire diameter was developed. Then the thermocouples were embedded into uncured propellant in a strand form. The temperature wave of this strand, burning in cigarette fashion, was recorded with the appropriate recording equipment. Once these steps had been accomplished, the traces obtained might then be analyzed in such a way as to investigate the surface temperature and general thermal behavior of different oxidizer particle size distributions, for several fuel compositions, and variations with combustion pressure.

CHAPTER II

REVIEW OF LITERATURE ON THERMAL STRUCTURE STUDIES

There are a large number of experimental techniques for the measurement of temperature profiles in combustion processes. All these methods can be classified into two groups: a) optical techniques and b) immersion probes.

Optical techniques allow a precise determination of temperature until very high values, but are limited to the gaseous phase only. Immersion probes present fluid-dynamic disturbances, and they are limited to relatively low temperatures.

However, due to the fact that the fundamental interest was in the solid phase of the combustion wave, the method of immersion probes was selected. From among these techniques it was evident that the one most suited was the thermocouple. The following discussion constitutes a brief review of the literature on temperature measurements related to the combustion mechanism of solid propellants.

A. Thermal Structure Measurements in Double Base Propellants

Klein, et al., (17), prepared fine thermocouples with Wollaston wires 12.5 microns diameter, of platinum and platinum-rhodium 10%. Thermocouples were placed between two half strands which were cut lengthwise and then cemented together with ethylacetate, and let dry for 6 days at 60° C.

The experimental temperatures were corrected for the difference between wire and gas temperature by extension of the method of Klaukens and Wolfhard (18), but the differences in temperature were so small as to be negligible. They report the presence of a catalytic effect of platinum wire, which was corrected by the use of borax coated thermocouples.

Assuming the general one-dimensional energy equation for steady state, and ignoring the heat generation term, they obtained for the solid phase

$$T - T_0 = (T_s - T_0) \exp\left(\frac{\dot{m} C_p x}{\lambda}\right) \quad [I-4]$$

where: T_0 = initial temperature of propellant
 T_s = surface temperature
 \dot{m} = mass burning rate
 C_p = specific heat
 λ = coefficient of thermal conductivity

Klein, et. al. plotted $\ln(T - T_0)$ vs. x and assumed that the point of departure from linearity defines the surface temperature, so long as heat generation does not become important until this point. They reported surface temperatures of the order of 250°C , and also found that an increase of pressure was accompanied by a narrowing of the wave and an increase in the flame temperature.

It might be pointed out that the deviation from linearity in the plot of $\ln(T - T_0)$ vs. x is very gradual. Thus, this could create certain inaccuracy in the readings, depending on what points are chosen to draw the straight line.

Another effect that may be noted is the smoothness of the temperature waves obtained. This is surprising since the physical change of phase should show up in a break of the trace.

Heller and Gordon (19) applied the same technique to another double base propellant. They reported no apparent change of the temperature gradient at the surface, which was interpreted as no abrupt change in the chemical reactions occurring in the foam and fizz zones. They observed a region of constant temperature between the sharp rise in temperature and the appearance of the flame, which was attributed to the induction zone. Spectrophotometric analysis of the combustion products in the induction zone, shows no change in composition with distance above the surface, and only minor changes with environmental pressure.

Different methods for determination of surface temperatures have been reported. Using a 5 grams weight, Heller and Gordon (19) pressed a platinum and platinum-rhodium 10% thermocouple, diameter 75 microns, against the surface during burning. Their results show a surface temperature of about 400 to 500° C. for the low pressure range, say 0 to 50 psig, a rapid increase with pressure up to 300 psig and from that point to 500 psig the surface temperature remains at about 1000° C. Care must be taken in interpreting these results because of the large size thermocouple employed. Especially at pressures higher than 300 psi, the thickness of the reaction zone is of the same order as the size of the thermocouple bead.

Powling (20) reported that the apparent surface temperature of cordites burning at atmospheric

pressure is in the range 500 to 700° C., using silica covered thermocouples.

Powling and Smith (21) applied an infrared technique to several double base compositions burning at atmospheric pressure. Their results agree with the low surface temperature values obtained by Klein, et al. (17).

Wilfong, Penner and Daniels (4) burnt a strand of double base powder, which had been mixed with very fine copper powder and then extruded, in a closed bomb and extinguished it by the rupture of a thin metal disc. A photomicrographic study showed that particles smaller than 4 microns had melted into spheres. Also, they found that the temperature was high enough to decompose finely divided calcium carbonate which had been incorporated into the propellant. Their results led them to postulate high temperatures of the order of 1000° C., for pressures of 1500 psi. It should be pointed out that at that pressure the flame is in close contact with the surface.

B. Thermal Distribution in
Liquid Nitrate Ester Strands

Related with these experiments in double base propellants are the ones conducted in liquid strands of stoichiometric mixtures of different nitrate esters. These compounds have ballistic and chemical properties similar to double base powders, and present, from the experimental point of view, certain advantages, i.e., smooth burning surface and transparency that helps to obtain a photographic record.

Hildenbrand, et al. (22) (23), applied a technique similar to the one developed by Klein, et al. (17), but worked with thermocouple wires of 7.5 microns diameter, employing micromanipulative techniques, and mounting the thermocouples into Pyrex tubes. High speed motion pictures were synchronized with the thermocouple records. Special interest was taken in the determination of the surface temperature. In order to expand the preheat zone as much as possible, their work was confined to the lower pressure region. Some typical results for ethyl nitrate are, at low pressure up to 200 psi the surface temperature is between 70 and 140° C., and for pressures between 300 and 900 psi the surface temperature is $155 \pm 10^{\circ}$ C.

Steinberger and Carder (24) employed similar technique and worked in the range of nitrogen pressures between 500 to 1000 psi for a range of similar compositions. They report surface temperatures of the order of ambient temperature. Work was done with thermocouple wires with and without borax coating, the difference being negligible. Finally, they postulated the necessity of a highly reactive free radical that diffuses back from the flame to attack the nitrate ester at the surface.

This last suggestion is the only one that differs from the generally adopted theory of feedback of heat from the gaseous zone to the surface as a controlling factor in the combustion process.

C. Thermal Wave Structure in
Solid Composite Propellants

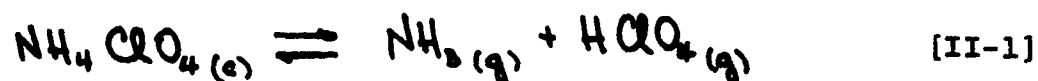
Attempts to study the temperature profile of solid composite propellants applying the technique described by Klein, et al. (17) have been reported.

Sutherland (2) embedded thermocouples made of platinum and platinum-rhodium 10%, wire diameter 12.5 microns, into small amounts of propellant mixture placed on a flat plate. After curing, the roughly circular flat test samples were cut into a strand form. The output of the thermocouple was fed into an oscilloscope and recorded by a 35 mm. drum camera. The emphasis of that work was on obtaining a temperature gradient at the surface. Three different mixture ratios of polyester-ammonium perchlorate were tested, as well as three different particle size distributions. The results indicated a slight steepening of the temperature gradient at the surface with pressure, and no significant variation with oxidizer particle size, or mixture ratio.

Nugent, Friedman and Rumbel (25), applying the same technique described before of embedding the thermocouples in thin sheets of propellant, reported thermocouple oscillograph traces together with high speed motion pictures. Their report shows some results with thermocouples of 25 microns wire for an Arcite type propellant of classified composition at 665 psi. In addition, they report attempts to embed thermocouples of 7.5 microns wire and smaller without success.

In the same report, Nugent, et al., refer to a classified paper (26), in which no success was found in applying the thermocouple method.

Powling and Smith (21) (27) apply another technique for the measurement of surface temperatures of burning ammonium perchlorate and weak fuel mixtures. An infrared emission method is applied at subatmospheric pressures. In addition, temperature distributions in the gas phase were recorded with thermocouples of 50 microns wire diameter. Results showed that, at any given pressure, the observed surface temperature was independent of the amount of fuel present, although large variations in burning rate were observed. The variation of surface temperature with pressure was similar for all fuel concentrations, although differences in surface temperature were found according to the vapor pressure of the fuel present, the temperature being higher for the fuels which were more difficult to gasify. They concluded that gas phase reactions control the rate of burning and that the surface reaction is the equilibrium process



Typical results for paraformaldehyde mixtures (10 to 24.3%) are:

p	T _s
mm. Hg.	°C
50	394
200	441
760	497

CHAPTER III

APPLICATION OF THERMOCOUPLE TECHNIQUE

This research was primarily an experimental one and included several phases. The reader will find a general outline of it in the next pages. Detailed description of some particular techniques can be found in the Appendices to this thesis.

A. Experimental Program

1. Thermocouple Fabrication

Wollaston wires of platinum and platinum-rhodium 10% of 7.5 microns diameter were cut in short lengths. The silver sheet was dissolved with nitric acid solution. Under a microscope and with micromanipulative technique, the bare tips of the wires were brought together. At this point a careful check of the presence of residues of silver was made so as to eliminate any possibility of secondary thermoelectric effect, as described in Appendix A.

The wires were then set forming an acute angle and the junction was welded with an acetylene-oxygen microtorch. Then the

thermocouple was carefully removed from the micromanipulators and stored in flat plates.

A complete description of the method is given in Appendix B. The experimental setup is shown in Figure 1.

2. Propellant

First attempts were made to glue the thermocouple in split half strands, but the glue line, made of the same composition as the strand, did not cure perfectly and also was not homogeneous in nature. As a consequence, it was decided to develop a technique for embedding the thermocouple directly into the uncured strand of propellant. As a start it was decided to pick a propellant with low viscosity and long curing time. These characteristics were presumed to be desirable for the embedding of the thermocouples.

A composition based on polybutadiene acrylic acid fuel and fine unimodal ammonium perchlorate, described as PBAA 70F, was considered to fulfill all the requirements. The fine oxidizer was considered most desirable for use with the fine thermocouples employed in this work. Table I gives the composition and physical data, while Figure 2 shows a plot of burning rate versus pressure for that composition.

In the latter stages of the research, bimodal oxidizer distributions were tested. Also, the effect of addition of the catalysts Copper Chromite and Ferric Oxide were studied. Table I shows the compositions and Figure 2 gives the burning rate versus pressure for these mixtures.

The propellant was made at the existing facilities of the Solid Propellant Building of the Guggenheim Laboratories at Princeton University. Complete description of propellant processing can be found in Appendix C.

3. Embedding of Thermocouples

The vacuum mixed uncured propellant was cast into a gun pressure cartridge, see Figure 3. Then with the appropriate gun pressure the propellant was fed into the bottom half mold as shown in Step (1) of the sequence of pictures, in Figure 4, showing the technique employed. Then the thermocouple was very carefully placed on top of this half mold.

Wires and bead were positioned like an inverted V under a microscope. The fuse wire for camera starting was positioned, see (2). Then the upper portion of the mold was assembled and the rest of the propellant filled in, see (3). The mold was placed in an oven for the required curing time. After that, it was disassembled and the finished strand taken out. For detailed description see Appendix D.

For each batch of propellant 36 thermocouples were embedded. For wires of 7.5 microns diameter, after the whole process, the use of this technique gives a yield of 65% intact thermocouples. For wires of 2.5 microns diameter, the yield was only 17%. But it would seem that with more practice this can be greatly improved, since only two batches were made with the finest wires.

4. Experimental Apparatus

The recording instrumentation consisted of a Dual Beam Oscilloscope Tektronix Model 551, with Type 53/54D Amplifiers. The trace was recorded by means of a 35 mm. strip film Electronic Tube Camera Model SM-100, which allows a speed variation from 1.27 to 30,500 centimeters per minute, approximately. A built-in glow lamp produces time marks on the edge of the film. Another feature is the possibility of remote control operation. This was effected by a fuse wire placed before casting the strand 2 to 3 mm. in front of the thermocouple bead. When the fuse wire melts due to the flame, the take-up reel is started. The film used was Kodak Tri X 35 mm. film, Type TX 417, in 100 foot rolls. Figure 5 is a picture of the instrumentation employed. This setup can be used to obtain records of the temperature profile of the combustion wave.

In the earlier tests it was found, in several cases, evidence of the emergence of some

point of the wires other than the bead. This was attributed to movement of the wires during casting, and could be avoided by very careful control of casting procedure. The effect encountered was, in some cases, simple breakage of the wires, and in other cases was a thermo-electric generation arising from the silver sheath of the Wollaston wire. These difficulties are fully described in Appendix A.

In the latter part of this work, some experiments were conducted to obtain another experimental indication of the surface temperature. To do this it was thought that a probe technique based on the differences in conductivity between solid and gas could be used. By such a procedure the passage of the probe through the surface might produce a sudden change of the signal in a suitably designed circuit. A complete description of this so-called "conductance probe" can be found in Appendix E. Figure 6 is a schematic representation of the experimental assembly.

5. Strand Burner

The strand with the embedded thermocouple is burned in cigarette fashion under nitrogen pressure in a chimney type bomb apparatus. One hole is drilled in the top of the strand by means of a very fine drill, and the ignition wire is inserted through it. A hole is drilled in the base of the strand so it can be vertically mounted on a pin of the strand burner. The ignition wire

is a Nichrome wire of the type used in a Parr bomb. The wire used to start the camera is a lead fuse wire of $\frac{1}{2}$ ampere capacity, and cast into the strand as mentioned previously.

The strand is mounted in the base of the strand burner, and the electrical connections are made. The thermocouple wires are soldered, using five core solder 60 Tin/40 Lead, to the insulated strand burner leads. Figure 7 shows a picture of the strand ready to be fired before the chimney is mounted.

The bomb is pressurized to the required level. A flow of nitrogen, controlled at the exit by an orifice, is maintained throughout the burning of the strand. The tests were conducted at ambient temperature, 22° C. The nitrogen control system and electrical controls are shown in Figure 8. The pressure in the strand burner is measured with bourdon type gauges.

The strand is ignited by applying 24 volts DC across the Nichrome wire. As the flame passes through the fuse wire, a relay is actuated and starts the takeup reel. After a couple of seconds the strip camera is stopped manually.

Also in the same apparatus, the burning rate measurements were made for conversion of the temperature versus time records to temperature versus distance. The procedure can be found in detail in references (14) and (15).

Due to the frequent breakage of thermocouple wires at pressures above 200 psig, the

continuous flow burner was abandoned. At higher pressures the tests were performed in a closed strand burner described in reference (14) and adapted to this purpose, see Figure 9. The thermocouple was mounted in the strand burner head as shown in Figure 10. Otherwise, all the procedures remained the same.

6. Double Base Experiments

In order to check the experimental apparatus, it was decided to do a series of tests with a double base propellant. The experimental results from such a propellant are abundant in the literature as has been seen before. The propellant was provided by Picatinny Arsenal in large sheets 3 millimeters thick. The sheets were cut in strands 6 x 100 mm.

Little pieces of propellant are dissolved in acetone to form a viscous solution. This solution is applied to one face of a strand and the thermocouple is placed very carefully over wet surface thus formed. Under the microscope the thermocouple is placed in the desired position, an inverted V, with a sharp hook. The surface then dries with the bead fixed in the forward position. Following this, another layer of the acetone-propellant solution is applied on top of the dried surface and also to one side of another strand. The two wet surfaces are then set together and the glued strand is put under pressure from a weight. It then is placed at 40° C., and allowed to dry for a week.

B. Determination of Surface Temperature

The principal aim of this work was the determination of the surface temperature, and two methods were applied. One of them is the so-called "conductance probe" already mentioned, but unfortunately it was not possible to develop this technique successfully.

The other method is based on comparing the experimental data with the one-dimensional steady-state heat balance equation at the surface. If we assume the model of Figure 11 where the solid propellant is moving into the flame zone at a constant velocity v from the left ($x < 0$) to the right ($x > 0$). The process is at constant pressure, i.e., we neglect the small change in pressure. The gases are ideal. The coefficient of thermal conductivity, λ , and the specific heat of the solid, c_p , are assumed independent of temperature. The solid is treated as a homogeneous reacting medium, which is true for double base, but questionable for composite propellants. Thermal and mass diffusion are present in the gas phase, and there is no mass diffusion in the solid. The heat balance equation in any plane of the combustion wave is given by

$$\frac{d^2T}{dx^2} - \dot{m} c_p \frac{dT}{dx} + \dot{q}_x = 0 \quad \text{[III-1]}$$

where: x = distance from burning surface.
 \dot{m} = mass burning rate
 \dot{q}_x = rate of heat release due to chemical reaction in the x-plane.

The other symbols have their usual meaning. The first term represents the rate of change in heat content due to conduction, and the second term is the rate of change of heat content due to mass flow.

If we further assume that exothermic reaction occurs at the surface, no reaction in the solid, then equation [III-1] becomes:

$$\frac{d^2T}{dx^2} - \dot{m} c_p \frac{dT}{dx} = 0 \quad \text{[III-2]}$$

Equation [III-2] can be integrated, see Appendix F, to give:

$$T - T_0 = (T_s - T_0) \exp\left(\frac{\dot{m} c_p x}{\lambda}\right) \quad \text{[III-3]}$$

where: T_s = surface temperature
 T_0 = initial temperature of propellant
 T = temperature at x-plane

and the other symbols have their usual meaning.

A plot of $\ln(T - T_0)$ vs. x gives a straight line. The point of departure from linearity is taken to be the surface temperature, due to changes in thermal diffusivity.

Also, from the plot of $\ln(T - T_0)$ vs. x the coefficient of thermal conductivity for the preheat zone on the solid can be deduced from the slope of the straight line.

C. Data Reduction

The 35 mm. film with the latent image of the temperature vs. time is processed, according to Kodak specifications, in a Morse tank for 100 ft. rolls. At the beginning the traces were read with a Recordak Microfilm Reader Model MPE. But later it was found more convenient to make 28 x 36 centimeter prints of the first rise of the trace. Figure 12 shows the steps involved in obtaining temperatures from the film record. The time marks on the edge of the film are produced by an AR-4 Argon timing lamp that flashes at line frequency (60 cycles). Each cycle is marked by vertical lines in the figure, which are then subdivided with a Gerber Variable Scale, Model TP 007100B, into several points marked on top of the trace. The reading is done in centimeters with the Gerber scale, and later transformed to millivolts by means of the calibrated gain used in the input amplifier to the scope. The millivolt reading is converted to temperatures with a National Bureau of Standards Circular 561 Table. Since the reference was ambient temperature, 22° C., it is necessary to add 0.113 MV to the voltage obtained before transforming into temperature. Table II shows the calculations performed for the test of Figure 12. From that table are taken the figures to plot $\log (T - T_0)$ vs. time as shown in Figure 13. Note that the abscissae are in cycles, and that to transform to time, they must be multiplied by 16.67 $\frac{\text{msec}}{\text{cycle}}$. By use of the appropriate burning rate the distance is obtained.

D. Measurement Limitations

1. Remarks on Thermocouple Technique

Before the interpretation of the results, a few remarks should be made about applying the thermocouple technique. The thermocouple represents the most direct method of measuring the thermal structure of the combustion wave, since it gives results for the solid phase as well as the gaseous phase of the wave. As Hunt (28) points out, the fine wire thermocouple is the smallest fabricated temperature transducer possible, and wires as small as 2.5 microns diameter have been used in this work.

But the following inconveniences should be taken into account: (i) the wires melt upon arriving at the hotter region of the flame; (ii) disturbances of the burning process due to local fluid dynamic effects are possible; (iii) heat conduction along the thermocouple wires could give erroneous results; (iv) heat radiation from the bead to its surroundings could affect the readings; and (v) catalytic effects of the platinum wire on the chemical reactions in the flame could occur. Problem (i) is almost overcome by the use of high melting point wires, like platinum and its alloys with rhodium, with which the temperature rise can be recorded almost completely. Problems (iii) and (iv) are considered negligible with very fine wires and very small beads, like the ones employed in this work as described previously. Problem (ii) and (v) are not present for the first part of the wave until

the surface of the solid is reached, so they are not taken into account. Furthermore, the catalytic effect has been reported negligible for the gaseous zone in references (19), (22), and (24). Nonetheless, it was planned, as part of this research, to check any possible catalytic effects by the use of borax or silicone coating of the thermocouple, provided there was sufficient time. At the time of this writing this had not been done.

2. Surface Temperature

The extreme steepness of the temperature gradient at the surface and the finite size of the thermocouples renders the surface temperature determination subject to error due to the thermal lags involved. This has been pointed out by Thies (29), who also analyzed this situation. A simple calculation will show the magnitudes of that error.

For the model assumed, the temperature gradient in the solid near the surface is given by

$$\left(\frac{dT}{dx}\right)_{x=x_s} = \frac{\rho r c_p}{\lambda} (T_s - T_o) \quad [\text{III-4}]$$

taken average values: $\rho = 1.6 \frac{\text{g}}{\text{cm}^3}$

$$r = 0.25 \frac{\text{cm}}{\text{sec}}, \quad c_p = 0.3 \frac{\text{cal}}{\text{g}^\circ\text{C}}$$

$$\lambda = 9 \times 10^{-4} \frac{\text{cal}}{\text{cm sec}^\circ\text{C}}, \quad T_s = 600^\circ\text{C}, \text{ and}$$

$T_o = 22^\circ\text{C}$, the temperature gradient at the

surface is of $8^\circ/\mu$ and across the thermocouple bead which is 1.7 times the wire diameter, or 12.7 microns for a 7.5 microns diameter wire, the temperature drop will be approximately 100° C.

The identification of the surface, as a definite point, has then no physical meaning. Furthermore, the size of the thermocouple bead is a factor that affects the thermal lag, thus becoming another addition to the uncertainties already involved.

3. Coefficient of Thermal Conductivity

The thermal lag influence is also evident for the calculation of the coefficient of thermal conductivity. As a consequence, λ will depend on the particular size of the thermocouple bead used in each test. Besides, the dependence of λ on burning rate makes the statistical distribution of oxidizer particles very important, since burning rate is dependent on oxidizer-fuel ratio and, under the microscopic point of view, these variations could account for a difference in λ .

E. Type of Results Expected

The comparison of records of double base composite propellant traces should show the difference in physical structure between the two classes of material. Furthermore, the surfaces of double base propellants are expected to be microscopically smooth, with the possibility of chemical reaction in the so-called "foam zone". Therefore, it is

reasonable to expect a very well-defined value for surface temperature. On the other hand, the heterogeneity of the composite materials should show up beginning in the solid, and be evident in different values for surface temperature according to the thermocouple position with respect to the distribution of oxidizer crystals and fuel pockets, in agreement with the "two temperature" description (3).

Another feature that could be detected is the flame heterogeneity of composite propellants. The following events might occur. In the solid there is no reaction. At the surface the propellant components vaporize. Now, the gaseous pockets of fuel and oxidizer mix by diffusion and after that they experience chemical reaction. In agreement with that scheme the thermocouple might show temperature variations corresponding to the position of the bead relative to the hot points created by oxidizer rich pockets.

Also, it is expected that information on the dependence of T_s on pressure could be obtained. Only semiquantitative values for the pressure region below 200 psi could be expected, since at higher pressures the narrowing of the wave will make the readings very inaccurate.

Variations of T_s with composition are expected to appear, especially when catalysts are added to the propellant. This would be interesting to check because of the possibility of explaining the effect of catalyst on burning rate by a lowering of surface temperature. The assumption made is that the presence of catalyst lowers the activation energy of the propellant, thus making it react even at low surface temperatures.

CHAPTER IV

RESULTS

The application of the method described before to the temperature-time records obtained for several mixtures of PBAA-ammonium perchlorate and for one double base propellant show the following results.

A. Surface Temperature

For the composition PBAA 70F, with which the bulk of the research was performed, a surface temperature of about 600° C. was measured. Within the sensitivity of the method, no variation of surface temperature with pressure was detected. The average values for each pressure are given in Table III.

Particular records for that composition are shown in Figures 14A, 15A, 16A, and 17A. The last one was made with a thermocouple of 2.5 microns diameter wire. Note that the rippling is much more accentuated as was expected with these very fine wires. This created some additional uncertainty in the determination of the surface temperature. Another interesting feature is the fact that the length of these ripples is approximately equal to the oxidizer average particle size.

The respective plots of $\log (\tau - \tau_0)$ vs. distance are shown in Figures 14B, 15B, 16B, and 17B. The surface temperatures thus obtained are tabulated in Table IV. These values of T_s are then indicated in the respective record. In general, these points

coincide with an evident break in the shape of the trace, except for Figure 17A, for reasons already mentioned.

A bimodal composition, PBAA 75BM, was tested at 15 and 30 psig. Figure 18A is a typical trace for this material, and Figure 18B is the respective plot of $\log (\tau - \tau_0)$ vs. distance. The average surface temperature for this composition is 540° C., and no variation with pressure was observed. The length of the ripples are longer in this case than for the unimodal very fine oxidizer composition. Measured values are tabulated in Tables III and IV.

Other propellants tested were the ones described by PBAA 70F 1C and PBAA 70F 1FO, both mixtures are substantially the basic composition PBAA 70F with the addition of 1% of catalyst, see Table I. The average values of the surface temperature for these materials are reported in Table III.

Also included in Table III are the average values of the surface temperature for a double base composition. Figures 19A and 20A are two typical traces. The correspondent plots of $\log (\tau - \tau_0)$ vs. distance are in Figures 19B and 20B. The values encountered agree well with the data reported by Klein, et al. (17).

B. Coefficient of Thermal Conductivity

The average values of λ obtained, as has been described above, are contained in Table III for the different propellants tested.

For the traces shown in Figures 14A to 18A, the correspondent values of λ are detailed in

Table IV. These values vary between 5 and 12×10^{-4}
 $\frac{\text{cal}}{\text{°C. cm sec}}$ for compositions PBAA 70F and PBAA 75 BM.

Comparatively, compositions with catalyst give coefficients of thermal conductivity which are twice those values, see Table III.

In general, it is observed that λ increases with pressure, this effect being more noticeable for the propellants having catalyst added.

For the double base propellant the average values of λ are contained in Table III, and they agree fairly well with the data cited in the literature (17).

C. Comparison of Double Base and Composite Propellant Temperature Profiles

The double base traces show a very smooth profile for all pressures. In contrast, however, the composite ones are rippled. This rippling being more accentuated for lower pressures than for higher pressures.

The rippling effect was more evident with thermocouples made from 2.5 microns diameter wires, see Figure 17A. The readings are quite different from point to point because of the irregular distribution of oxidizer particles. The thermal lags involved are much lower than for the 7.5 micron wires, and consequently the probe is more sensitive, giving this apparently wild trace.

Also, comparison of these traces with the ones obtained from a bimodal particle size distribution of the oxidizer, Figure 18A, shows that the rippling is larger for the bimodal than for the unimodal, which indicates influence of the oxidizer particle size on the shape of the combustion wave.

D. Gas Temperature

After the steep initial rise, in which the rippling is evident, the temperature attains a constant value and the rippling tends to disappear. This plateau temperature is below the melting point of the thermocouple wires, which is lower than the estimated flame temperature. The level of this plateau temperature increases with pressure. In general, the plateau ends suddenly when the thermocouple breaks, but in the last tests of this program, which were performed on a composition PBAA 70F 1C, (similar to the one used in the bulk of this research, but with the addition of 1% of copper chromite catalyst), it was observed in certain cases that the trace shot up to values higher than the melting point of the thermocouple wires. The length of the plateau, until the second rise of temperature appears, is of the order of 2.2 mm. at 400 psig, and 2.0 mm. for 1000 psig.

This effect suggests the possibility of a "second stage" flame, but there is not enough evidence to establish it. Much needs to be done before the possibility of errors is eliminated and good reproducibility of the phenomenon is obtained. Thus, no explanation is offered of this effect at the present moment.

For the double base propellant a similar plateau appears, but the temperature level is lower for same pressures, and agrees well with the expected value of the "dark zone" temperature.

CHAPTER V

DISCUSSION AND CONCLUSIONS

A. Differences Between Double Base and Composite Propellants

1. Physical Interpretation

The contrast between the smooth temperature profiles of the double base propellant and the rippled ones obtained with the composite mixtures was not surprising. This observation is in agreement with the different physical nature of the propellants.

The double base composition is basically a colloidal suspension of nitrocellulose and nitroglycerin with the oxygen in the same molecule, and can be assumed to be perfectly homogeneous. It enters the flame as a premixed solid that has been heated to the surface temperature by heat conduction.

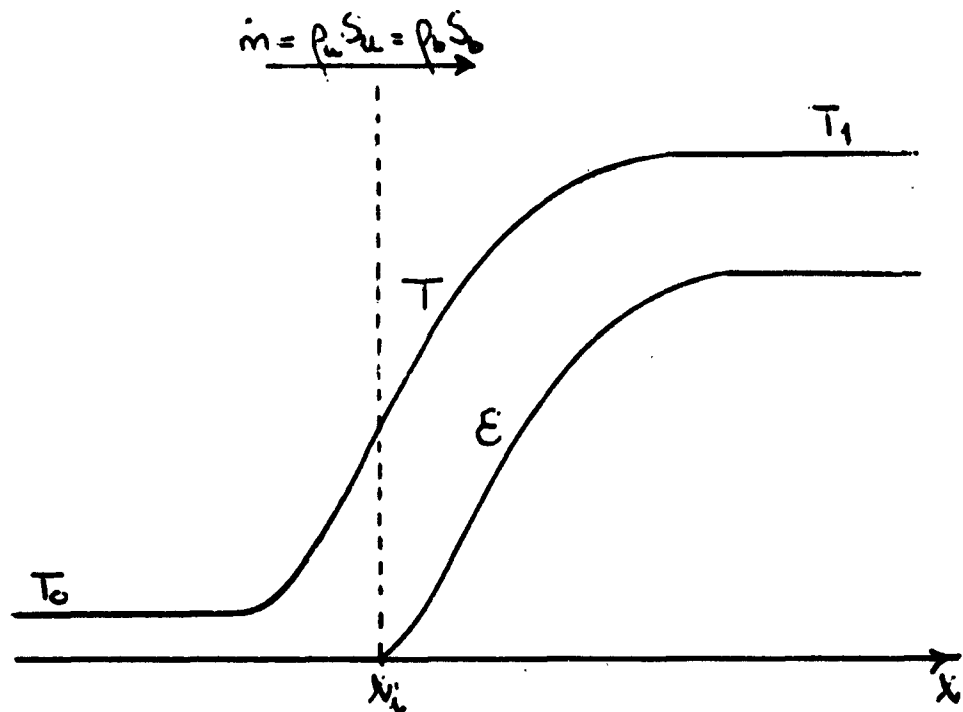
In contrast to this, composite propellants are heterogeneous mixtures of inorganic oxidizer crystals and organic fuel binder. Consequently, the heat conductivity in the solid preheat zone between the thermocouple bead and the surface will be affected by the statistical distribution of the oxidizer crystals. In the gaseous zone adjacent to the surface of composite propellants, there is mixing by diffusion of both components and the chemical reaction starts only after a certain time lag. This effect can be detected by the difference in breakaway points at the surface, in confronting both classes of propellants.

2. Analysis

Comparison between the logarithmic plots of temperature vs. distance for a double base propellant, Figures 19B and 20B, and composite mixtures, Figures 14B to 18B, shows a noticeable difference in the shape of the temperature profile at the surface breakaway point.

Analysis of the possible factors that can influence the shape of the temperature profile in a laminar flame (30) shows the following facts:

a) Case I - Consider the classical model of a premixed gas, with thermal diffusion and mass diffusion, assume one-dimensional steady flow; and no solid phase present. The energy equation for the model pictured in sketch V-1:



Sketch V-1

can be written as

$$\frac{\lambda}{\dot{m} c_p} \frac{dT}{dx} = (T - T_0) - \xi (T_1 - T_0) \quad [V-1]$$

where: ξ = fraction of the flow rate
that is the product
 x_i = phase where ignition takes place
The other symbols have their usual meaning.

Dividing both sides of equation [V-1] by $(T - T_0)$ and defining a fractional temperature rise:

$$\theta = \frac{T - T_0}{T_1 - T_0}$$

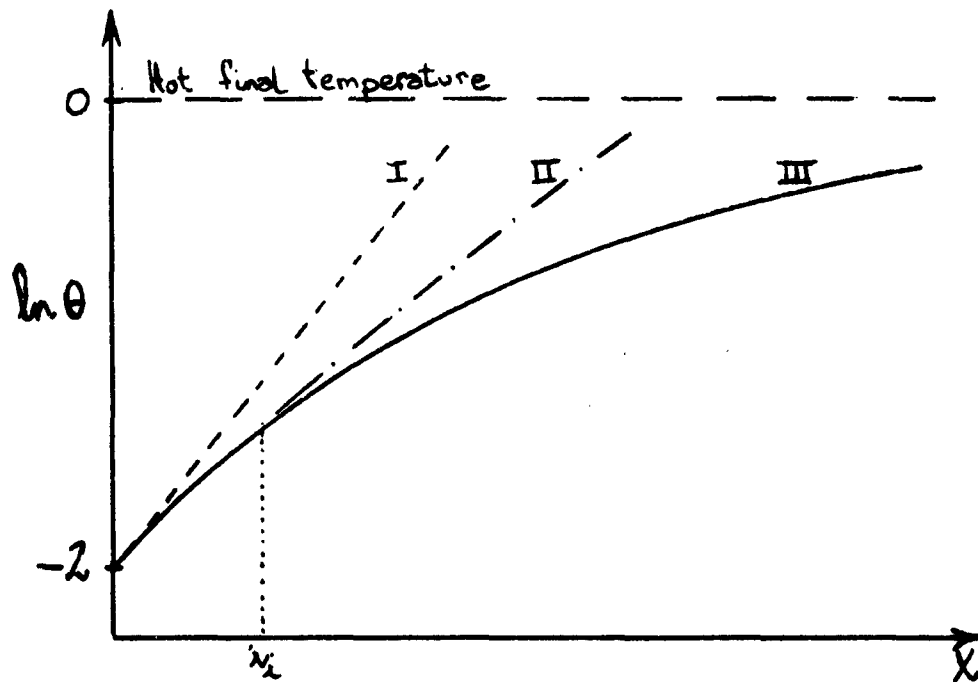
the energy equation becomes:

$$\left[\frac{\lambda}{\dot{m} c_p} \right] \frac{d(\ln \theta)}{dx} = \left(1 - \frac{\xi}{\theta} \right) \equiv R \quad [V-2]$$

The values of the right side R at different phases of the profile will be:

- a) at $x = x_i$ is $\xi = 0 \therefore R = 1$
- b) at $x = +\infty$ is $\xi = 1, T = T_1 \therefore R = 0$
- c) and R diminishes from 1 to 0 as x goes from x_i to ∞ . The plot of $\ln \theta$ vs. x shows that $\frac{d(\ln \theta)}{dx}$ is steep before the place where reaction starts, and it declines from then on. Furthermore, the multiplier $\left[\frac{\lambda}{\dot{m} c_p} \right]$ is proportional to $T^{1/2}$, this meaning that the slope

of the logarithm diminishes going from the cold to the hot side. These facts are shown in the following sketch V-2:



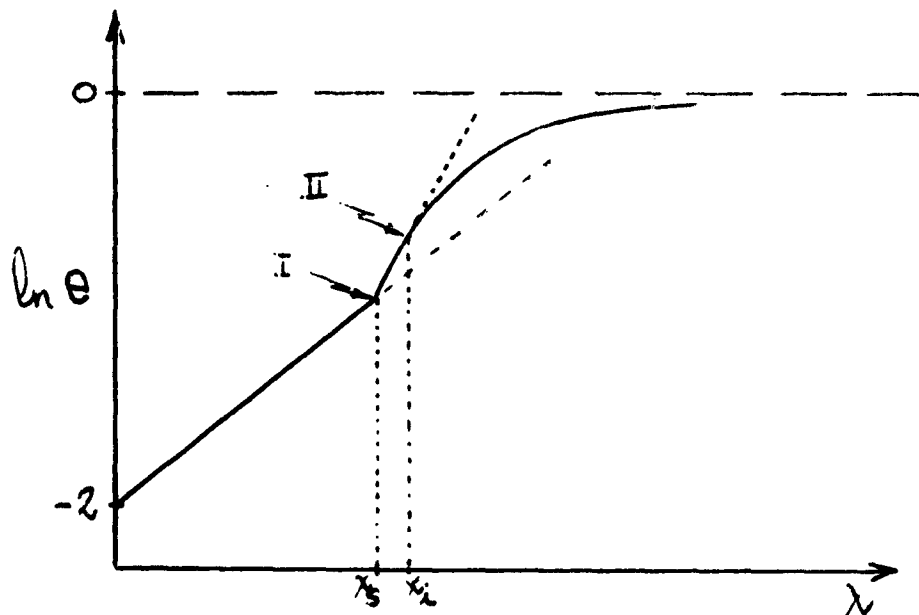
Sketch V-2

- where:
- (I) is a straight line, for constant λ and no reaction taking place.
 - (II) is a curved line, due to variations in λ and C_p , and no reaction occurring.
 - (III) is the real curve with reaction starting at point x_i where the breakaway bends downward.

b) Case II - Apply now this reasoning to a premixed solid propellant, with thermal and mass diffusion in the gas phase, and no mass diffusion in the solid, i.e., just a plain heat conductivity model. Consider exothermic decomposition occurring

at the surface, but assume that active reaction starts at a distance $x_i \geq 0$ from the surface. Following is sketch V-3 showing the corresponding plot of $\ln \Theta$ vs. x , assuming that the reaction starts at a certain distance from the surface, and for $\lambda_{\text{gas}} < \lambda_{\text{solid}}$ in agreement with:

$$\lambda_g \left(\frac{dT}{dx} \right)_g = \lambda_s \left(\frac{dT}{dx} \right)_s - \dot{m} Q \quad [\text{V-3}]$$



Sketch V-3

Note that in this case there are two breaks in the curve:

- (I) at the solid surface due to change in coefficient of thermal conductivity, and then
- (II) at "ignition" point where the active reaction starts. In consequence, the steepest zone between the solid surface and the beginning of the reaction is a pure gas conduction zone with no chemical reaction.

Application of these reasonings to the temperature vs. time records of double base and composite propellants, as is shown in Figures 21 and 22 respectively, indicates that chemical reaction might start at the surface for double base compositions. This does not seem to be the case for composite mixtures.

B. Surface Temperature

There is enough evidence to ascertain that the surface temperature is around 600° C., for the special composite propellants tested during this work.

No variation of surface temperature with pressure was detected, and also no variation with propellant composition, as is shown in Table III, T_s being approximately the same for the propellants described as PBAA 70F, PBAA 75 BM, PBAA 70F 1C and PBAA 70F 1FO. A possible explanation for this could be the following. The thermocouple bead is always covered by a film of fuel. Then, according to the "two-temperature" postulate, what the thermocouple probably reads is the surface temperature of the fuel.

Also, it must be pointed out that in the case of compositions with catalyst addition, the reading of T_s will be less reliable, due to increase of thermal lag, as has been pointed out before.

Powling and Smith (21), (27) applied a radiometric technique to the determination of surface temperature for ammonium perchlorate-fuel mixtures at low pressure. They obtained surface

temperatures in the neighborhood of 500° C. Considering the difference in material and techniques, this result is in good agreement with those of the present work.

The values of T_b for the double base propellant are similar to the ones obtained by Klein, et al. ($\sim 250^\circ\text{C}$)(17). Since the same method was used for their measurement, analogous limitations apply for their interpretation, as was pointed out in Chapter II.

C. Coefficient of Thermal Conductivity

The values of λ for the composite propellants show a large scattering. This can be attributed to the heterogeneous physical structure of the material, which creates for each test a different path for the thermal wave between thermocouple bead and propellant surface. Furthermore, λ depends on burning rate, and this on oxidizer-fuel ratio. Then, considering that the length of the preheat zone in the solid is only of the order of 100 μ it is possible to have effects due to the oxidizer crystals distribution, which affect the microscopic burning rate. Also, the possibility of burning rate variation from batch to batch of propellant must be pointed out.

There is an apparent increase of λ with pressure, as indicated by Table III. But, this is possibly due to thermal lag influence, which increases with burning rate, and this with pressure. Figure 23 shows average values of λ vs. burning rate for the different compositions tested.

Nonetheless, the values obtained agree fairly well with similar data found in the literature, e.g., Medford (31) reports

$\lambda = 9.8 \times 10^{-4} \frac{\text{cal}}{\text{C. cm sec}}$ for a PBAA-ammonium perchlorate propellant.

CHAPTER VI

RECOMMENDATIONS

The uncertainties involved in the determination of T_s could be eliminated by the development of an auxiliary tool like the "conductance probe" outlined in Appendix E.

A better attempt could be to investigate the pressure range of interest in rocket propulsion. To do that the use of thermocouples of 2.5 microns diameter or less would be mandatory.

On the other hand, the possibility of spreading the combustion wave at subatmospheric pressures, would diminish the thermal lag considerably. Thus, providing the opportunity of investigating the strong dependence of T_s on pressure, as reported by Powling and Smith (21) and (27).

The possibility of catalytic effect of the thermocouple wires should be checked with borax or silicone coatings.

The nature of the moderately high temperature plateau, and the possibility of a "two stage" flame should be investigated by the use of high melting point thermocouples. Tests in small rocket motors should be performed, in order to reproduce normal conditions of combustion. In that way the possibility of interference of the cold nitrogen flow in the strand burner, as was used in this work, would be eliminated.

Of interest will be the results obtained with a single oxidizer, ammonium perchlorate and different

fuels. And conversely tests should be conducted on a single fuel, polybutadiene-acrylic acid, and different oxidizers. In each case the effect of pressure, initial temperature, oxidizer particle size, mixture ratio and catalyst addition, should be analyzed.

Appendix A: Secondary Thermoelectric
Effect on Wollaston Wires

Platinum is a very ductile metal. Directly from it can be obtained wires as fine as 20 microns diameter. For smaller sizes it is convenient to employ the Wollaston procedure (32), by which the platinum wire is covered with a silver sheath, and then drawn through wire dies of the required size. This process allows the obtaining of platinum wires as small as 0.5 micron. For thermoelectric measurement purposes that silver sheath must be eliminated to allow the two noble metals to contact and form the bead. Initially, in order to obtain more strength in manipulating the wires, the silver attack with nitric acid solution in water (1:1) was made over 3 mm. length of the wires. The thermocouple bead was formed, and the finished thermocouple was embedded into the strand.

Some of the early results indicated that the flame approached the silver coated wire first rather than the bead. This was due to movements of the thermocouple wires either while the mold assembly was performed or during the curing process.

That this was the case was demonstrated by bringing a hot metal near a single Wollaston wire of platinum, which was bare in the middle for a length of approximately 10 cm. The two extremes of the wire were connected to the scope in the usual way. When the hot metal approached to the middle, no variations were observed on the scope; but when the hot wire approached one of the ends of the silver sheath the scope showed a deviation of approximately 2 millivolts.

When the hot metal was brought near to the other end of the silver sheath, the deflection obtained was of the same magnitude, but in the opposite direction.

To overcome this effect some efforts were directed at obtaining thermocouples with fine ceramic holders. From all trials the one that took the least time was the following. The wires were attacked to dissolve 6 mm. of silver sheath. The platinum wires were inserted through single hole ceramics and cemented with sauerisen, and the same steps were taken with the platinum-rhodium 10% wires. The ceramics were 1 mm. internal diameter, 1.5 mm. external diameter and 40 mm. long. One of the extremes showed only bare wire, the silver sheath being completely inside the ceramic. For identification purposes each ceramic was given a code color. The sauerisen was allowed to dry one day.

The ceramics with the wires were handled in a similar manner in the micromanipulators as the wires above. Once the bead was formed, the ceramics one by one were deposited very carefully in a plate holder, this step gave large breakage of thermocouples. Then the ceramics were brought together, glued with Duco cement, and let dry.

The process was too time consuming, and since we had enough experience at this point with the direct manipulation of the wires, it was decided to attack the silver sheath for a length of 6 mm., which was thought to be enough to be safe from the secondary thermoelectric effect. To check this, several x-ray pictures were taken. Figure 24 shows a typical picture slightly improved to show the bare wires. In all the cases the position of the wires was similar to the position at the moment of embedding the thermocouple.

Appendix B: Thermocouple Production Technique

Initial attempts were performed with 12.5 microns diameter wire until enough experience was obtained. Then the bulk of the work was done with 7.5 microns wires and some with 2.5 microns wires.

One of the objectives was to obtain reproducible beads which were as small as possible in order to reduce thermal lag to a minimum. Earlier attempts were performed with a butt-welding technique, in which the wires were positioned under a microscope by means of a fixed stand with clip forceps holding one wire and another clip forceps as the arm of a Misco micromanipulator. With the tips of the wires just touching, the wires were connected to a circuit that when closed produced a discharge of a preset variable voltage, thru a capacitance that was also variable. The success with that method was poor and the beads obtained considered mechanically weak. The final method adopted was microtorch welding.

The Wollaston wires of platinum and platinum-rhodium 10% need to be cleaned of the silver sheath that the Wollaston process (32) adds to them. Pieces of platinum wire 5 cm. long and platinum-rhodium 10% 6.5 cm. long are cut, the difference being to help identification. The silver is dissolved in lengths of approximately 6 mm. by immersion in a solution of 1 part nitric acid and 1 part distilled water. After attack the wires are washed in distilled water and let dry.

Then the wires are clamped in a pair of Hagenbarth surgery clip forceps which act as the arms of precision instrument micromanipulators Misco and

Brinkmann, both having three degrees of freedom, see Figure 1.

The bare tips of the wires are now positioned under a "Stereozoom" microscope, Bausch and Lomb, set for low magnification (7X). The arms of the micro-manipulators are brought together until the wires are almost touching and form an angle of 45 to 60° between them. The microscope is then zoomed to high magnification (30X). Before final setting, the flame of the microtorch is passed lightly over the bare wire just to make sure that, if any silver is present, it will be melted and carried away from the tip. This operation must be very carefully controlled, because of the possibility of secondary thermoelectric effect due to the presence of silver, see Appendix A. The wires are then reset in the position previously described and with intermediate magnification (20X) the junction is welded with an acetylene-oxygen microtorch (Misco) with a tip number 000 that gives a flame approximately one-half millimeter wide and one millimeter high. When this flame is held near the junction the red color attained by the wires indicates the condition at which optimum welding can be made.

The thermocouple beads obtained are almost spherical with an average diameter 1.7 times that of the wire for 7.5 micron wires, and 2 times wire diameter for wire of 2.5 microns diameter. Then the thermocouple is smoothly deposited directly from the holders to a black painted plate, care being taken to keep the wires in the same position that they have in the micromanipulators. Finally, the plate is put on a rack which holds ten of these plates, separated by spacers 8 mm. high, that can be seen on the

background of Figure 1. The rack is wrapped with aluminum foil until the moment of embedding the thermocouple arrives.

Appendix C: Propellant Processing

The following description applies to mixture PBAA 70F, with which the bulk of this research was performed. The composition is detailed in Table I.

Propellant mixing was carried out in a double arm Z-blade mixer manufactured by Atlantic Research Corporation. The optimum capacity for that mixer is 300 grams. When burning rate determinations were also necessary, the mixing was performed in a Readco Overlapping Arm Laboratory Mixer of one gallon capacity.

The first step was the weighing of the required amount of ammonium perchlorate from plastic bags inside a sealed drum. The perchlorate is placed in a grinding hammer mill, and by varying hammer speed, feed rate and the number of passes, the required particle size distribution can be obtained. The relatively low combustion limit of the mixture with very fine oxidizer was not a problem because we were interested in a spreading of the preheat zone in the solid, so the tests were to be conducted at pressures below 200 psig.

The fuel was prepared by weighing the necessary amounts of PBAA and Epon 828, mixing them thoroughly in a beaker, and then placing them into the mixer. The oxidizer was placed on the pan of a Syntron Corporation vibratory feeder. From that time all the mixing operation was conducted by remote control. First the mixer was started, and then the oxidizer was slowly fed by careful control of the vibrator. Once the oxidizer was all added, the vacuum cap was positioned in top of the mixer and the mixing was continued under vacuum, 5 mm. Hg,

for 20 minutes. During mixing the propellant temperature was maintained at 56° C. After mixing, a small amount of propellant was poured in a beaker and its viscosity checked with a Brookfield Viscosimeter.

The propellant was cast thru a funnel in top of a vacuum desiccator which fed the propellant through a slit-shaped opening of 1/8" into both a gun pressure cartridge placed inside the desiccator, see Figure 3, and blocks for burning rate measurements.

Then the molds for burning rate determinations were wrapped in aluminum foil and placed in the oven and cured for 48 hours. The gun cartridge was taken for the thermocouple embedding process.

Appendix D: Embedding of Thermocouples

The vacuum mixed, uncured propellant is cast thru a slit-shaped opening on top of a desiccator into a gun pressure cartridge with a good quality rubber balloon, contained in the desiccator, see Figure 3.

The molds are coated with a thick layer of silicone vacuum grease, which acts as a release agent, and are kept in the oven at 80° C. for a half hour before casting in order to increase the fluidity of the grease, and also to help the feeding of the propellant into the molds.

The succeeding technique is shown in the sequence of steps of Figure 4. First, with the gun at a pressure of air of 80 to 120 psi, depending on viscosity of mixture, the uncured propellant is fed into the lower half mold (1) then is sent back to the oven for a short period of time, from which the molds will be taken one by one for the process of embedding the thermocouples.

Then, with one thermocouple in a plate beside the mold, the platinum-rhodium 10% wire is carefully picked up with very fine tweezers while the platinum wire is held with a sharp Tyrell iris hook, the whole assembly is smoothly translated from the plate to the top of the lower half of the mold that contains uncured propellant, care having been taken that the position of the wires remains with the original approximately 45° angle between them, since this helps to position the bead on the tip of an inverted V over the thermocouple. Under a stereo microscope (Spencer) the wire positions

are corrected with help of the hook. Finally, the wires are slightly pushed into the surface of the propellant to insure complete wetting, so that they will remain in that position. The 1/2 ampere lead fuse wire for camera starting is placed 2 to 4 mm. in front of the bead (2). The upper portion of the mold is then put in place and the rest of the propellant is inserted (3), care being taken that the propellant is fluid enough not to create stresses that can break the thermocouple. The entire assembly is placed in a laboratory oven and cured for the required time and temperature, after which the mold is taken out of the oven and disassembled before it cools off. The strand is then carefully taken out (4). Next, the strand is rinsed in water for 10 minutes and let dry. After checking continuity with an ammeter, the strand is stored in a closed cabinet until the moment of use.

Appendix E: Conductance Probe as an
Auxiliary Tool for Surface Indication

Because of the uncertainties involved, in the thermocouple measurements, it would be good to have another way of determining the physical property considered. Since this work was primarily concerned with measurements of surface temperature, the idea of an electric conductance probe was born.

The idea is to embed a Nichrome wire into the strand, insulated from the thermocouple by the dielectric properties of the propellant. One of the thermocouple wires is biased with a positive potential. The two legs of the probe are fed into one of the channels of a dual beam scope, the other channel being the thermocouple trace recorder.

The moment the bead emerges into a gaseous zone, the ionized gas in contact with the surface should close the circuit with the Nichrome wire already in the gas. The high electrical conductivity should be recorded by a sharp rise on the scope. By superimposing the two traces, the position of this rise would mark the location of the surface on the temperature curve. A schematic representation of the instrumentation used is shown in Figure 6.

Unfortunately, the technique was not successful. The current rise generally occurred before the thermocouple trace started. These spurious signals will take detective work to correct. Nevertheless, it is suggested that its use as an auxiliary tool for the accurate determinations of T_s would be extremely convenient if it could be perfected.

An interesting related phenomena was observed when the thermocouple wires break. The record obtained

indicates the presence of a plasma thermocouple which continues to deliver E.M.F. The wild fluctuations of the trace thus obtained are possibly related to the ionized granular flame.

Appendix F: Solution of Heat Balance Equation [III-2]

For the simplified model assumed, Figure 11, the heat balance equation was reduced to:

$$\frac{d^2T}{dx^2} - \dot{m} c_p \frac{dT}{dx} = 0 \quad [\text{III-2}]$$

The two boundary conditions to apply to this second grade equation are: first, at the solid surface, $x = 0$, the temperature will be the surface temperature; and second, deep in the solid, $x = -\infty$ the temperature will be the initial temperature of the propellant.

Then rewriting equation [III-2] like:

$$\frac{d}{dx} \left(\frac{dT}{dx} \right) - \frac{\rho r c_p}{\lambda} \left(\frac{dT}{dx} \right) = 0$$

Replacing $\left(\frac{dT}{dx} \right) = p$

$$\frac{dp}{dx} - \frac{\rho r c_p}{\lambda} p = 0$$

Rearrangement gives:

$$\frac{dp}{p} = \frac{\rho r c_p}{\lambda} dx$$

Integrating once:

$$p = C_1 \exp\left(\frac{p r c_p}{\lambda} x\right) = \frac{dT}{dx}$$

$$dT = C_1 \exp\left(\frac{p r c_p}{\lambda} x\right) dx$$

Second integration gives final solution:

$$T = C_2 \exp\left(\frac{p r c_p}{\lambda} x\right) + C_3$$

Applying boundary conditions:

$$\begin{aligned} \text{at } x = -\infty \quad & \text{is } T = T_0 \\ & \text{and } e^{-\infty} = 0 \\ & \therefore C_3 = T_0 \end{aligned}$$

Replacing:

$$T = C_2 \exp\left(\frac{p r c_p}{\lambda} x\right) + T_0$$

$$T - T_0 = C_2 \exp\left(\frac{p r c_p}{\lambda} x\right)$$

$$\begin{aligned} \text{at } x = 0 \quad & \text{is } T = T_s \\ & \text{and } e^0 = 1 \\ & \therefore C_2 = T_s - T_0 \end{aligned}$$

Finally:

$$T - T_0 = (T_s - T_0) \exp\left(\frac{p r c_p}{\lambda} x\right)$$

Appendix G: Commercial Equipment and Materials

I. Equipment

<u>Item</u>	<u>Manufacturer</u>	<u>Use</u>
1. Stereo-Zoom Microscope	Bausch and Lomb	Thermocouple Fabrication
2. Misco Micro-manipulator	Microchemical Specialties Company Berkeley, California	Thermocouple Fabrication
3. Brinkmann Micro-manipulator Type MPV, Clamp A	Brinkmann Great Neck, L.I., N.Y.	Thermocouple Fabrication
4. Misco Microtorch	Microchemical Specialties Company Berkeley, California	Thermocouple Welding
5. Dual-Beam Oscilloscope Textronix Model 551 Amplifiers Type 53/54D	Tektronix, Inc. Beaverton, Oregon	Thermocouple Output Measurement
6. ETC Scope Recording Camera Model SM-100	Electronic Tube Corp. Philadelphia, Pa.	Thermal Wave Recording
7. Recordak Microfilm Reader Model MPE	Recordak Corporation New York, N. Y.	Data Reduction
8. Gerber Variable Scale Model TP 007100B	Gerber Scientific Instrument Co. Hartford, Connecticut	Data Reduction
9. Z-Blade Double Arm Mixer, Model 35LP	Atlantic Research Corp. Alexandria, Virginia	Propellant Mixing
10. Readco Overlapping Arm Laboratory Mixer	Read Standard Corp. York, Pa.	Propellant Mixing
11. Bantam Mikro-Pulverizer, Type SH	Metals Disintegrating Company Summit, N. J.	Oxidizer Grinding
12. Syntron Vibratory Feeder, Model F-To	Syntron Corporation Homer City, Pa.	Oxidizer Feeding

Appendix G: Commercial Equipment and Materials-contd.

I. Equipment

<u>Item</u>	<u>Manufacturer</u>	<u>Use</u>
13. Pyles Sealant Gun	Pyles East Coast Co. Wilmington, Delaware	Propellant Casting
14. Brookfield Synchron- electric Viscosimeter, Model RVT, with Helipath Stand	Brookfield Engineering Laboratories Stoughton, Mass.	Propellant Viscosity Measurement
15. Reverse Action Clip Forcep	Falvey Co. Plainfield, N. J.	Thermocouple Manipulation
16. Sharp Tyrell Iris Hook	Falvey Co. Plainfield, N. J.	Thermocouple Manipulation
17. Fisher Isotemp Laboratory Oven	Fisher Scientific Co. New York, N. Y.	Propellant Curing and General Use

Appendix G: Commercial Equipment and Materials-contd.

II. Materials

<u>Item</u>	<u>Manufacturer</u>	<u>Use</u>
1. Platinum and Platinum-Rhodium 10% Wollaston Wires	Sigmund Cohn Mt. Vernon, N. Y.	Thermocouple Fabrication
2. Kodak Tri X 35 mm Film Type TX 417	Eastman Kodak Co. Rochester, N. Y.	Thermal Wave Recording
3. Single Hole Ceramic Insulators	Leeds and Northrup Philadelphia, Pa.	Thermocouple Fabrication
4. Ammonium Perchlorate Standard AMS-C66F	American Potash and Chemical Corp. Los Angeles, Calif.	Propellant Oxidizer
5. PBAA Polymer	American Synthetic Rubber Company Louisville, Kentucky	Fuel Binder
6. Epon 828	Shell Chemical Co. Emeryville, Calif.	Fuel Binder
7. Silicone Vacuum Grease	Dow Corning Corp. Midland, Michigan	Mold Release Agent
8. Copper Chromite	Harshaw Chemical Co. Cleveland, Ohio	Propellant Additive
9. Ferric Oxide	Baker Chemical Co. Phillipsburg, N. J.	Propellant Additive

REFERENCES

1. Geckler, R. D., "The Mechanism of Combustion of Solid Propellants", Selected Combustion Problems, Fundamentals and Aeronautical Application; AGARD Combustion Colloquium, Cambridge Univ., Butterworth's Scientific Publications, London, 1954, pp. 289-340.
2. Sutherland, G. S., "The Mechanism of Combustion of an Ammonium Perchlorate-Polyester Resin Composite Propellant", Ph.D. Thesis, Princeton University, May, 1956.
3. Schultz, R., Green, L., and Penner, S. S., "Studies of the Decomposition Mechanism, Erosive Burning, Sonance and Resonance for Solid Composite Propellant", Third AGARD Colloquium, 1958, pp. 367-430.
4. Wilfong, R. E., Penner, S. S., and Daniels, F., "An Hypothesis for Propellant Burning", Jour. Phys. and Coll. Chem., V. 54, 1950, pp. 863-872.
5. Crawford, B. L., Huggett, C., and McBrady, J. J., "Mechanism of the Burning of Double-Base Propellants", Jour. Phys. and Coll. Chem., V. 54, 1950, pp. 854-862.
6. Rice, O. K., and Ginell, R., "Theory of Burning of Double-Base Rocket Powders", Jour. Phys. and Coll. Chem., V. 54, 1950, pp. 885-917.
7. Parr, R. G. and Crawford, B. L., "A Physical Theory of Burning of Double-Base Rocket Propellants", Jour. Phys. and Coll. Chem., V. 54, 1950, pp. 929-954.
8. Rice, O. K., "The Theory of Burning of Rocket Powders", OSRD Report No. 5574, 1945.
9. Nachbar, W., "A Theoretical Study of the Burning of a Solid Propellant Sandwich", Solid Propellant Rocket Research, Academic Press, 1960, pp. 207-226.
10. Chaiken, R. F. and Andersen, W. H., "The Role of Binder in Composite Propellant Combustion", Solid Propellant Rocket Research, Academic Press, 1960, pp. 227-252.
11. Levy, J. B. and Friedman, R., "Further Studies of Pure Ammonium Perchlorate Deflagration", 8th Symposium on Combustion, Academic Press, 1961, pp. 663-672.

REFERENCES cont'd

12. Summerfield, M., Sutherland, G. S., Webb, M., Taback, H. J., and Hall, K. P., "Burning Mechanism of Ammonium Perchlorate Propellants", Solid Propellant Rocket Research, Academic Press, 1960, pp. 141-182.
13. Webb, M. J., "The Dependence of Linear Burning Rate Upon Pressure for Ammonium Perchlorate-Polyester Resin Composite Solid Propellant", M.S.E. Thesis, Princeton University, May, 1958.
14. Taback, H. J., "The Effects of Several Composition Factors on the Burning of an Ammonium Perchlorate Solid Propellant", M.S.E. Thesis, Princeton University, September, 1958.
15. Bastress, E. K., "Modification of the Burning Rates of Ammonium Perchlorate Solid Propellants by Particle Size Control", Ph.D. Thesis, Princeton University, January, 1961.
16. Powell, H. N., Fifth Symposium on Combustion, Reinhold, 1955, pp. 290-302.
17. Klein, R., Mentzer, M., von Elbe, G., and Lewis, B., "The Determination of the Thermal Structure of a Combustion Wave by Fine Thermocouples", Jour. Phys. and Coll. Chem., V. 54, 1950, pp. 877-884.
18. Klaukens, H., and Wolfhard, H. G., "Measurements in the Reaction Zone of a Bunsen Flame", Proc. Roy. Soc. (London), 193A, pp. 512-524.
19. Heller, C. A., and Gordon, A. S., "Structure of the Gas Phase Combustion Region of a Solid Double Base Propellant", Jour. of Phys. Chem., 59, 1955, pp. 773-777.
20. Powling, J., Selected Combustion Problems, AGARD, Butterworth's Scientific Publications, London, 1954, p. 389.
21. Powling, J. and Smith, W. A. W., "Measurement of the Burning Surface Temperature of Propellant Compositions by Infra-red Emission", Comb. and Flame, V. 6, 1962, pp. 173-181.

REFERENCES cont'd

22. Hildenbrand, D. L., Whittaker, A. G., and Euston, C. B., "Burning Rate Studies: I. Measurement of the Temperature Distribution in Burning Liquid Strands", Jour. of Phys. Chem., V. 58, 1954, pp. 1130-1133.
23. Hildebrand, D. L., and Whittaker, A. G., "Burning Rate Studies: II. Variation of Temperature Distribution with Consumption Rate for Burning Liquid Systems", Jour. of Phys. Chem., V. 59, 1955, pp. 1024-1028.
24. Steinberger, R. and Carder, K. E., "Surface Temperature of Burning Liquid Nitrate Esters", Jour. of Phys. Chem., V. 59, 1955, pp. 255-257.
25. Nugent, R. G., Friedman, R., and Rumbel, K. E., "Temperature-Profile Studies in Solid Propellant Flames", Atlantic Research Corp., AFOSR-TN-57-212, AD. No. 126509, March, 1957.
26. Aerojet General Corp., Report No. 649, V. 1 (Final), Azusa, California, (Feb. 1953), Confidential.
27. Powling, J. and Smith, W. A. W., "The Surface Temperature of Burning Ammonium Perchlorate", Report No. 10/R/62, E.R.D.E.
28. Hunt, M. H., "Design and Use of Fine Wire Thermocouples for Research", NOTS TP 1919, NAVORD Report 5828, September, 1959.
29. Thies, Ch. E., "Temperature Profiles of Solid Propellant Charges During Combustion", ARS Preprint 510-57, December 2, 1957.
30. Summerfield, M., Private communication, January, 1963.
31. Medford, J. E., "Measurement of Thermal Diffusivity of Solid Propellants", J. of A.R.S., V. 32, September, 1962, pp. 1390-1392.
32. Strong, J., Procedures in Experimental Physics, Prentice-Hall, New York, 1946, p. 542.

TABLE I

PROPELLANT COMPOSITIONS

Propellant Designation	COMPONENTS % WEIGHT					
	PBAA	Epon 828	AP FINE 9 μ	AP COARSE UNGROUND	COPPER CHROMITE	FERRIC OXIDE
PBAA 70F	25.7	4.3	70	-	-	-
PBAA 70F-1C	25.7	4.3	70	-	1	-
PBAA 70F-1FO	25.7	4.3	70	-	-	1
PBAA 75 BM	21.4	3.6	22.5	52.5	-	-

TABLE II

Calculation performed on test shown in Figure 12.

TIME	VOLTAGE		$T - T_0$
Cycles	cm	mv	$^{\circ}\text{C.}$
0.1	0.03	0.10	36
0.2	.04	.13	42
0.3	.08	.27	62
0.4	.08	.27	62
0.5	.10	.33	72
0.6	.12	.40	82
0.7	.13	.43	86
0.8	.15	.50	96
0.9	.17	.57	105
1.0	.20	.67	118
1.1	.21	.70	123
1.2	.24	.80	136
1.3	.32	1.07	169
1.4	.38	1.27	193
1.5	.45	1.50	221
1.6	.55	1.83	259
1.7	.65	2.16	295
1.8	.80	2.66	349
1.9	1.00	3.33	420
1.95	1.12	3.73	461
2.00	1.31	4.36	525
2.05	1.47	4.90	579
2.10	1.65	5.50	638
2.15	2.10	7.00	780
2.20	2.50	8.33	901
2.25	2.75	9.15	974
2.30	3.10	10.31	1073
2.35	3.20	10.66	1103
2.40	3.20	10.66	1103
2.5	3.50	11.65	1186
2.6	3.65	12.15	1227
2.7	3.75	12.50	1256
2.8	3.80	12.65	1269
2.9	3.90	13.00	1298
3.0	3.85	12.80	1287

TABLE III

Average values of T_s and λ for compositions described in Table I.

Propellant Designation	P psig	r mm sec.	Number of Deter- minations	T_s Range of Values	T_s av. °C.	λ Range of Values	$\lambda_{av.}$ cal 10^{-4} g C. cm sec
PBAA 70F	15	3.1	4	550-650	615	3.7-6.7	5.3
	30	3.3	15	550-670	612	3.7-13.2	7.1
	50	4.0	3	640-700	660	5.0-7.1	6.1
	100	4.8	12	490-650	583	5.4-13.7	8.4
	150	5.3	12	540-700	603	7.1-12.3	10.3
PBAA 70F-1C	15	4.4	2	600	600	10.7-11.0	10.9
	100	9.2	2	600-630	615	15.4-21.9	18.6
	200	12.3	3	530	530	18.4-19.9	19.1
	1000	22.1	5	510-550	532	25.4-39	31.0
PBAA 70F-1FO	15	3.8	2	550-560	555	5.2-16.0	10.6
	100	7.9	3	660-700	667	8.0-24.0	15.3
	200	10.9	2	460-560	510	17.0-21.0	19.0
PBAA 75 BM	15	1.7	4	500-600	538	4.8-6.6	5.5
	30	2.0	4	450-600	540	4.5-13.7	8.9
Double Base	50	2.7	8	250-350	332	4.2-10.9	7.2
	100	6.7	3	300-350	333	5.1-9.6	7.8
	150	8.4	4	250-280	268	6.4-12.8	10.7

TABLE IV

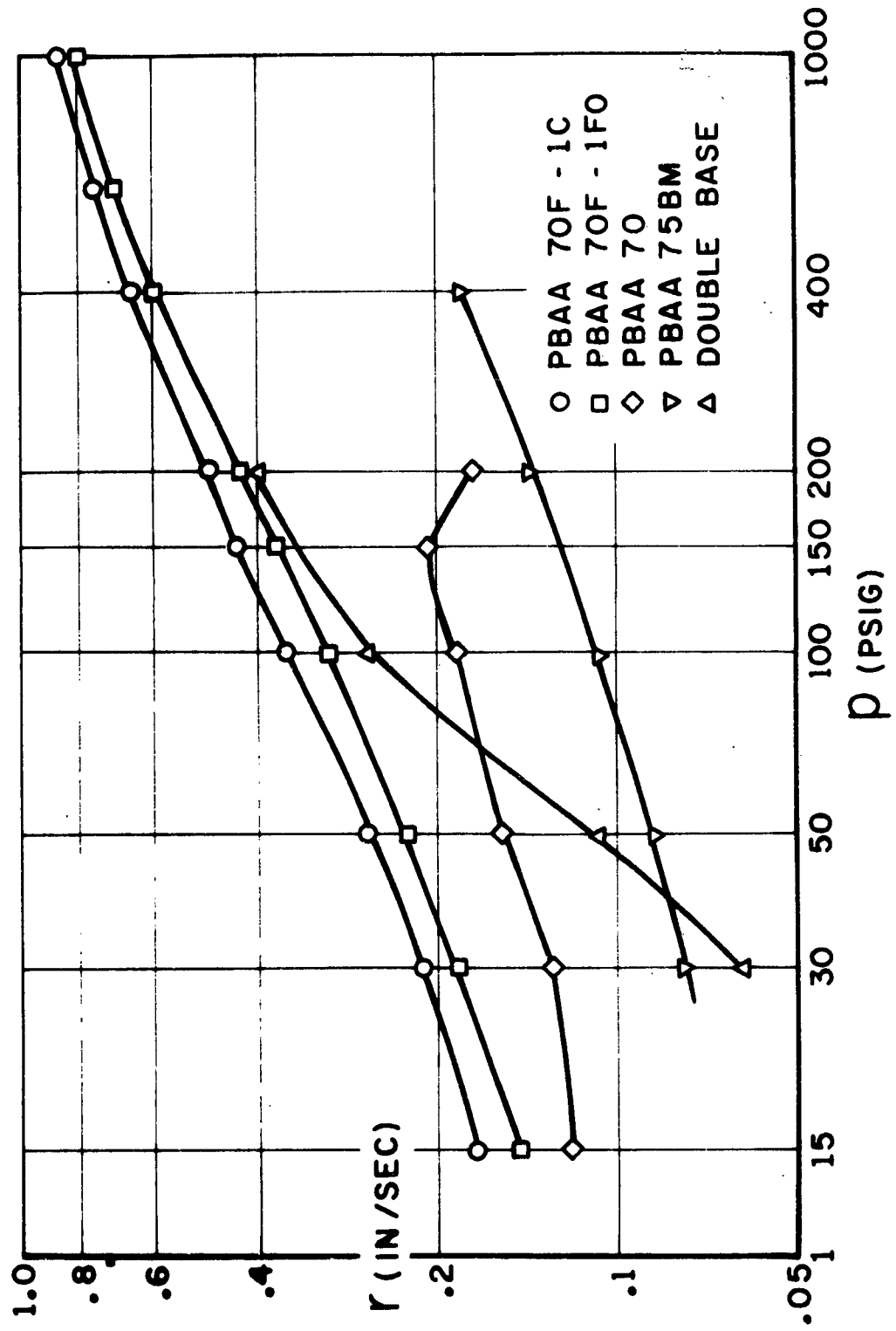
Values of T_s and λ for particular tests shown in Figures 14A to 20A.*

Figure	Propellant Description	Pressure psig	$\frac{r}{\text{mm}}$ sec.	T_s °C.	λ $10^{-4} \frac{\text{cal}}{\text{g C.cm sec}}$
14A	PBAA 70F	30	3.3	570	5.4
15A	PBAA 70F	100	4.8	560	7.3
16A	PBAA 70F	150	5.3	600	8.6
17A	PBAA 70F	30	3.3	550	6.3
18A	PBAA 75 BM	30	2.0	550	9.3
19A	Double Base	50	2.7	250	4.2
20A	Double Base	150	8.4	270	11.4

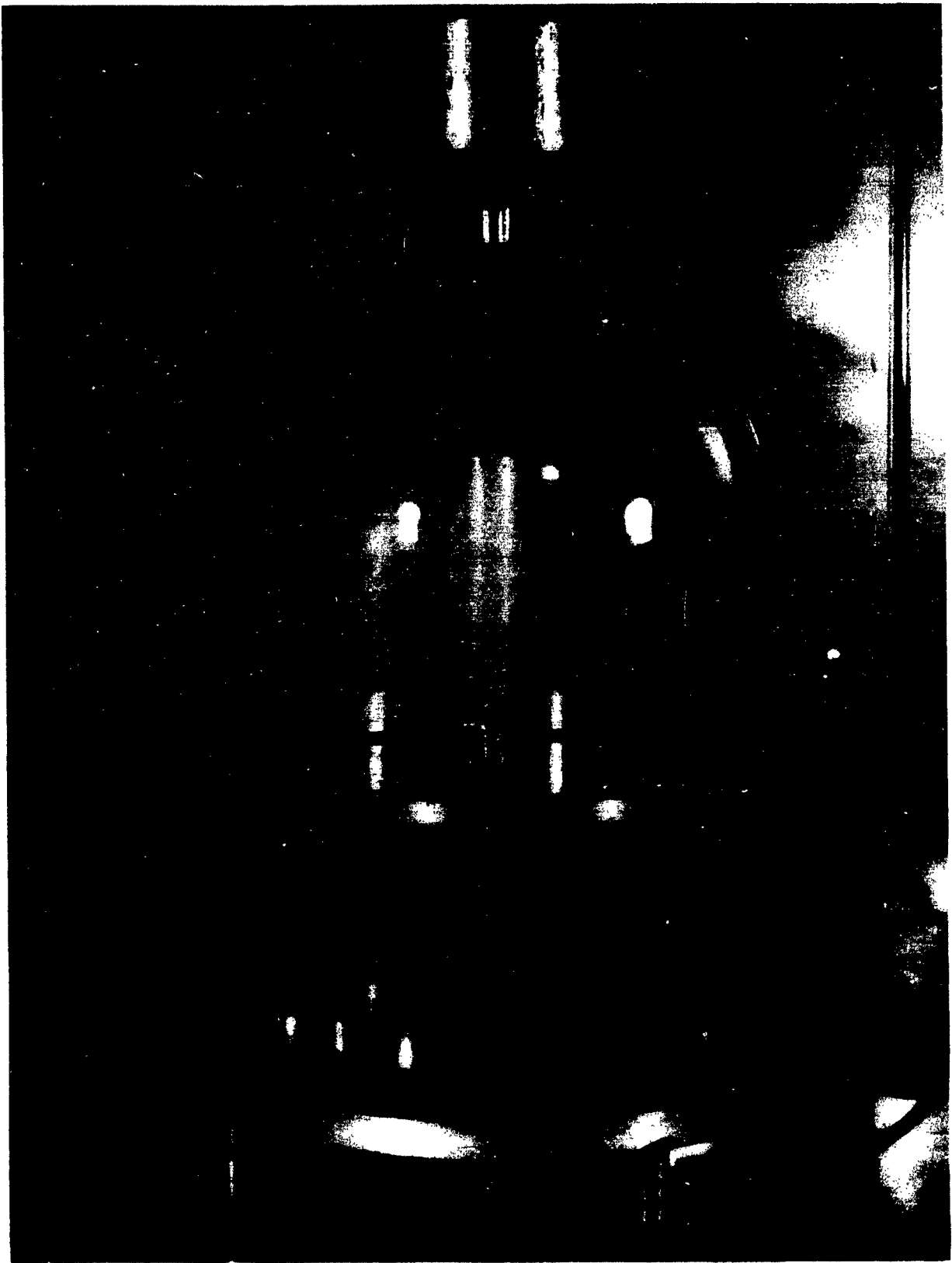
*The first column gives the figure number where Subscript A is a print directly from the 35 mm film. The same number with Subscript B is the corresponding plot of $\log (T-T_0)$ vs. X .



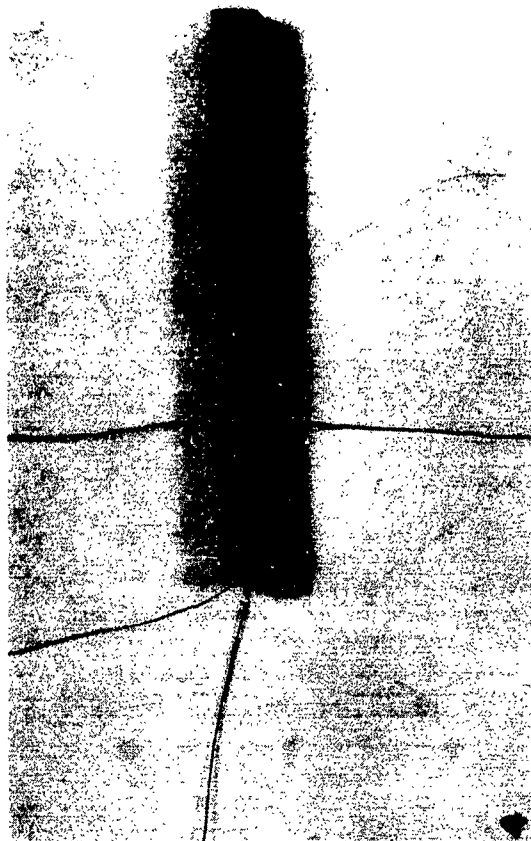
APPARATUS AND TOOLS EMPLOYED FOR FABRICATION
OF MICROTHERMOCOUPLE



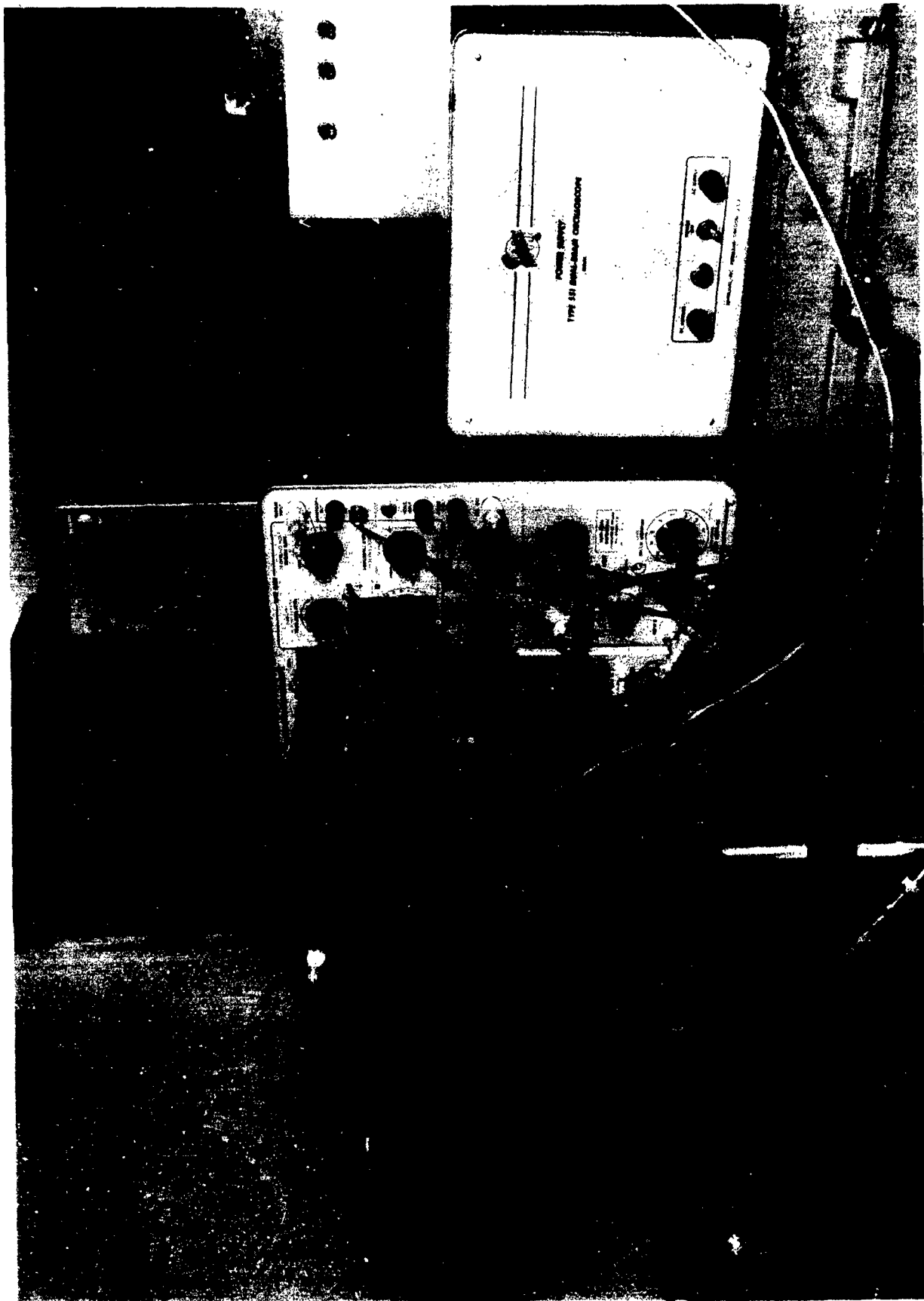
BURNING RATE VS PRESSURE FOR PROPELLANT COMPOSITIONS STUDIED



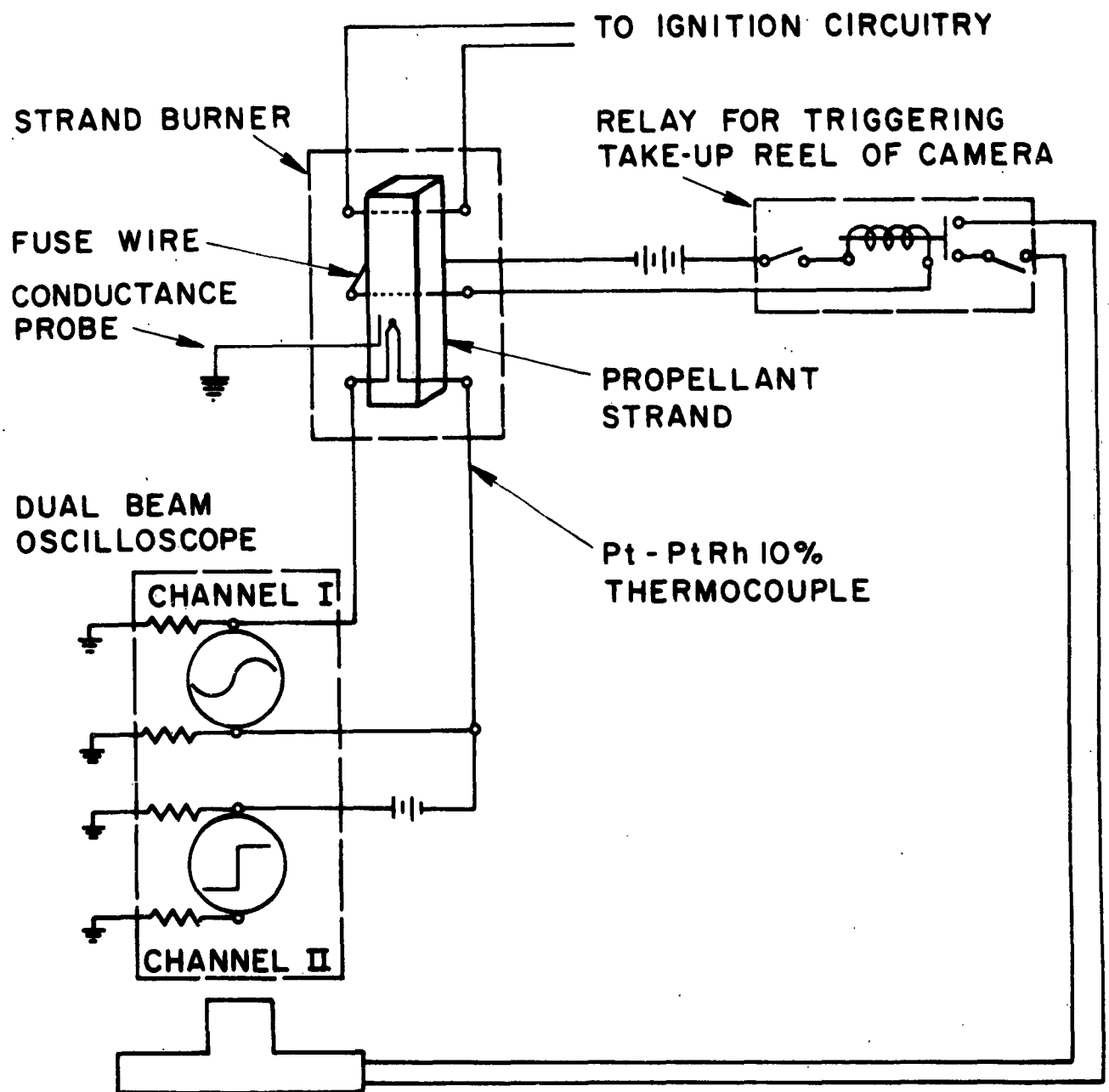
PROPELLANT CASTING APPARATUS



SEQUENCE SHOWING TECHNIQUE FOR EMBEDDING THERMOCOUPLE IN STRAND



ELECTRONIC RECORDING INSTRUMENTATION FOR THERMOCOUPLE TRAVERSES



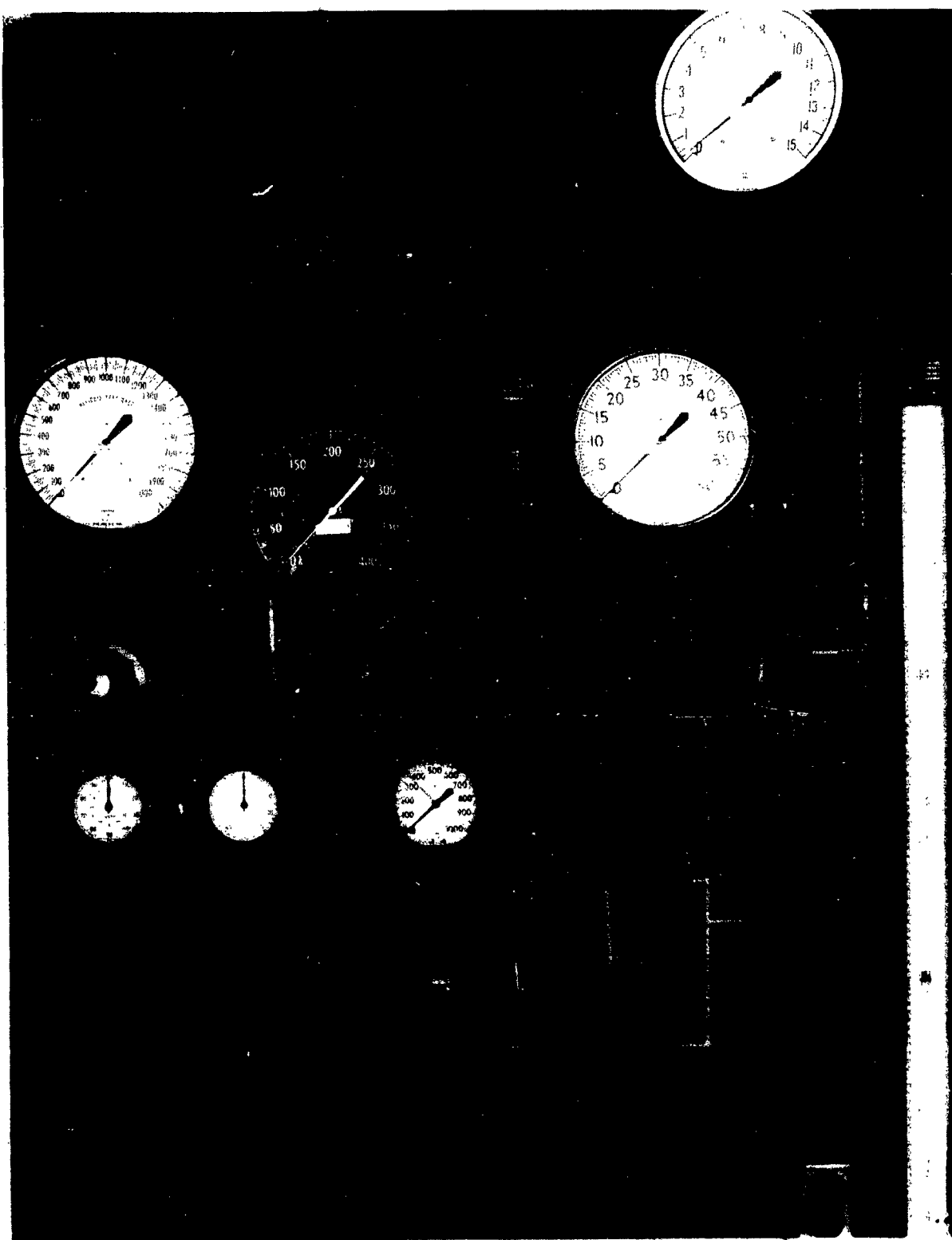
SCHEMATIC REPRESENTATION OF INSTRUMENTAL SET-UP FOR THERMOCOUPLE TRAVERSES

**CHANNEL I MEASURES THERMOCOUPLE SIGNAL
CHANNEL II MEASURES ONSET AT IONIZATION**

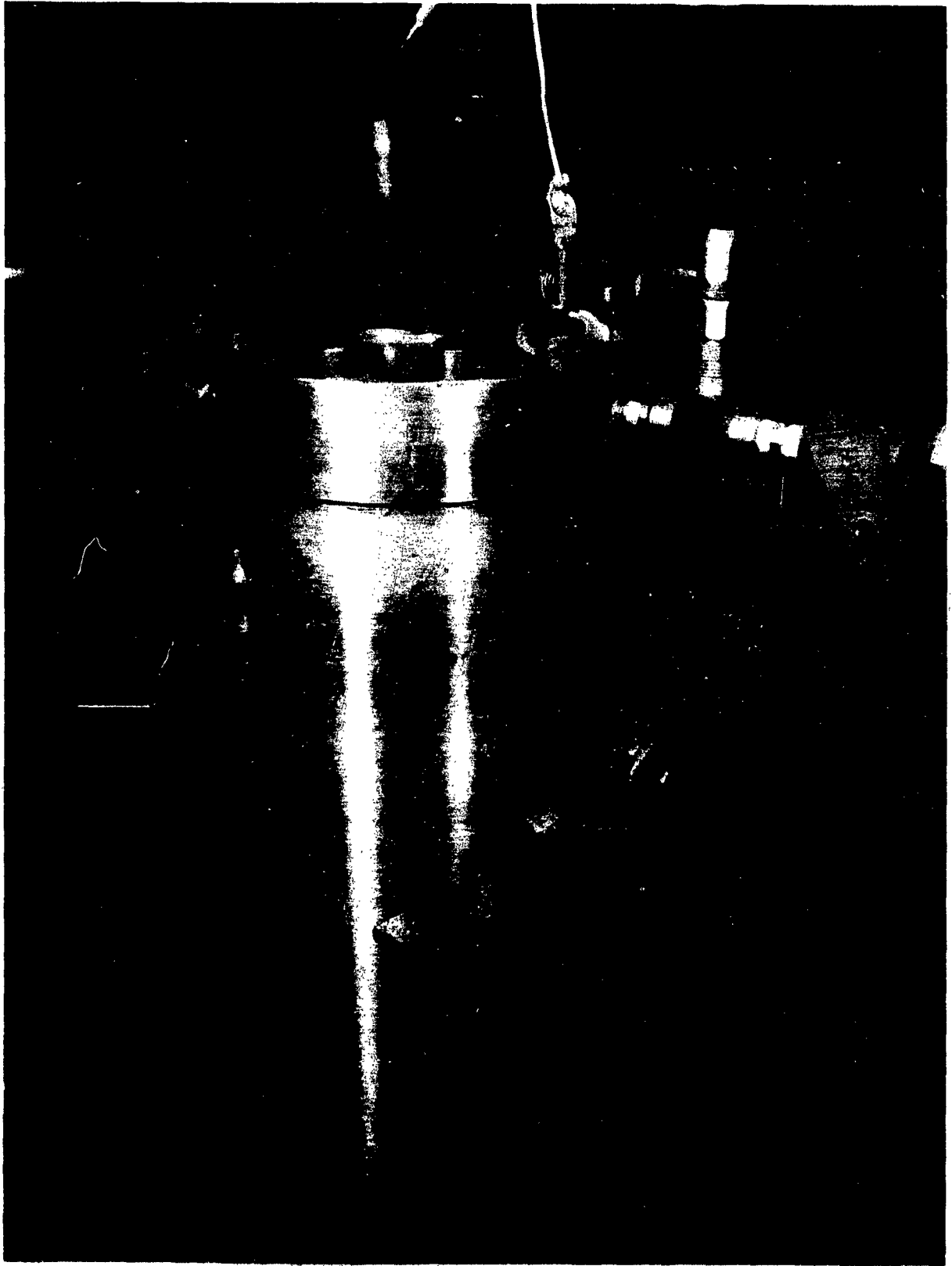
FIGURE 6



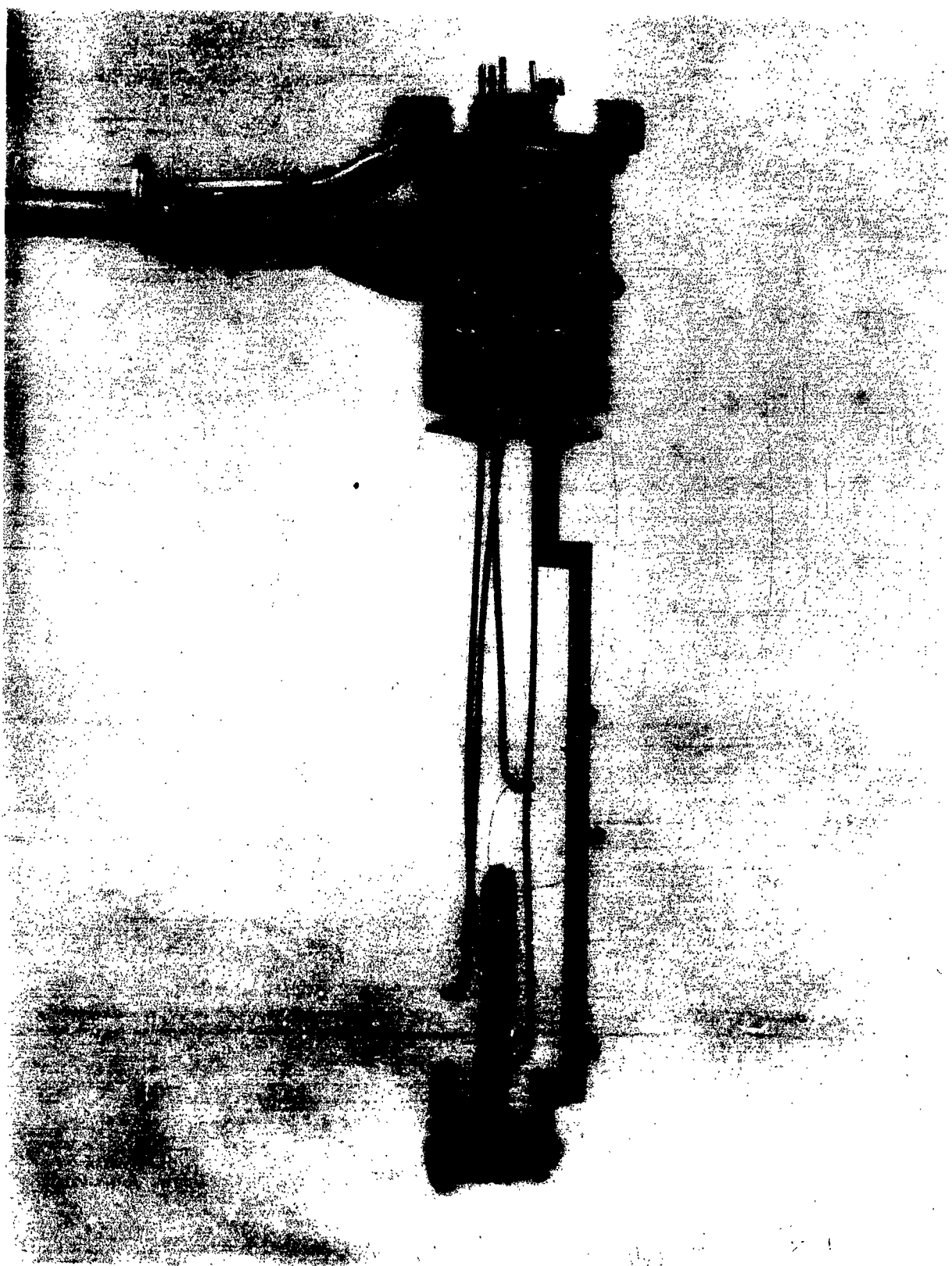
STRAND READY FOR TEST IN CHIMNEY STRAND BURNER



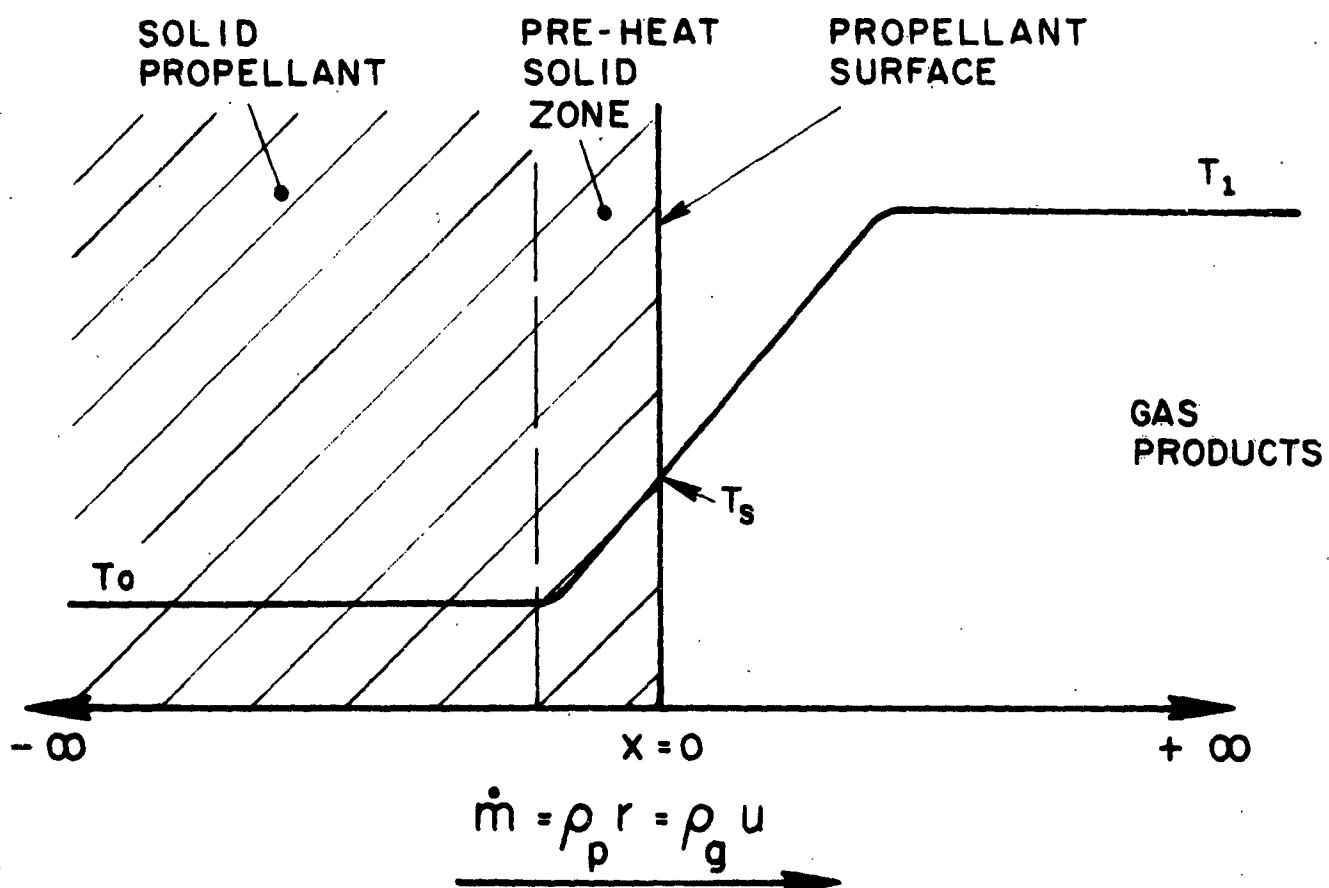
**CONTROL PANEL FOR STRAND BURNING
RATE APPARATUS**



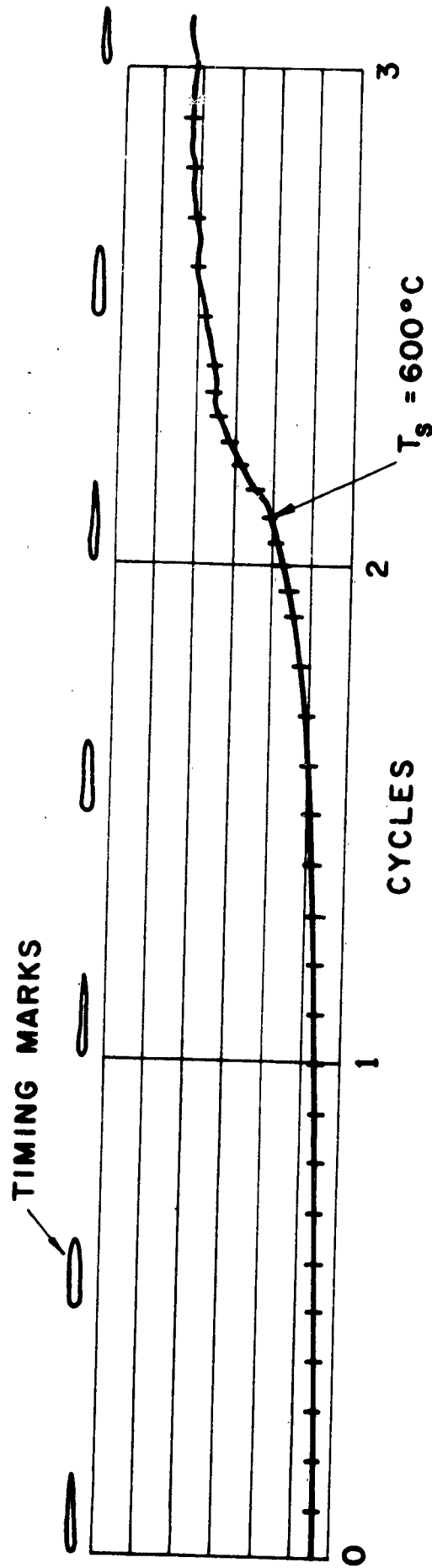
STRAND BURNER



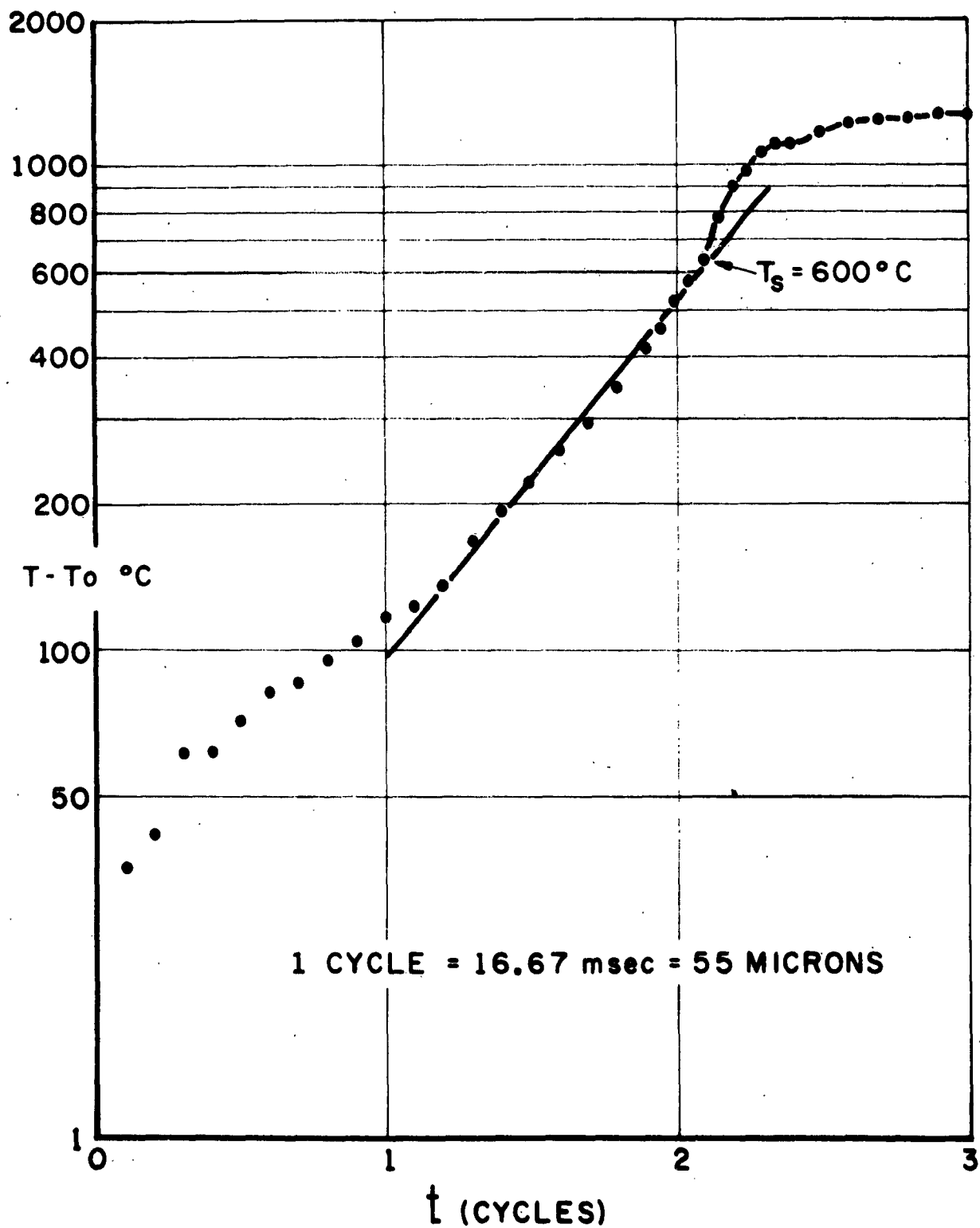
STRAND HOLDER PREPARED FOR A TEST



MODEL OF ONE-DIMENSIONAL
STEADY-STATE BURNING



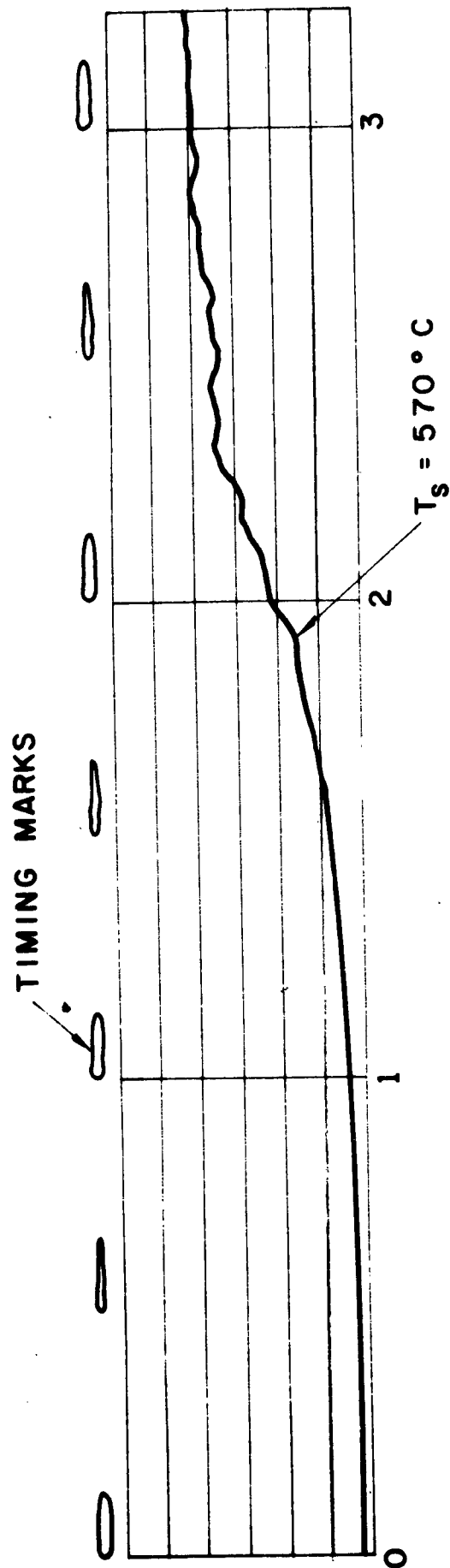
VOLTAGE - TIME RECORD FOR PROPELLANT COMPOSITION PBAA 70F,
 SHOWING METHOD OF OBTAINING DATA. NITROGEN PRESSURE
 30 PSIG. ONE HORIZONTAL DIVISION EQUALS 3.33mv. DISTANCE
 BETWEEN VERTICAL LINES CORRESPONDS TO ONE CYCLE = 16.67 msec.



PLOT OF LOG (T-T₀) VS TIME CORRESPONDING
TO TEST SHOWN IN FIGURE 12
DATA FROM TABLE II

FIGURE 13

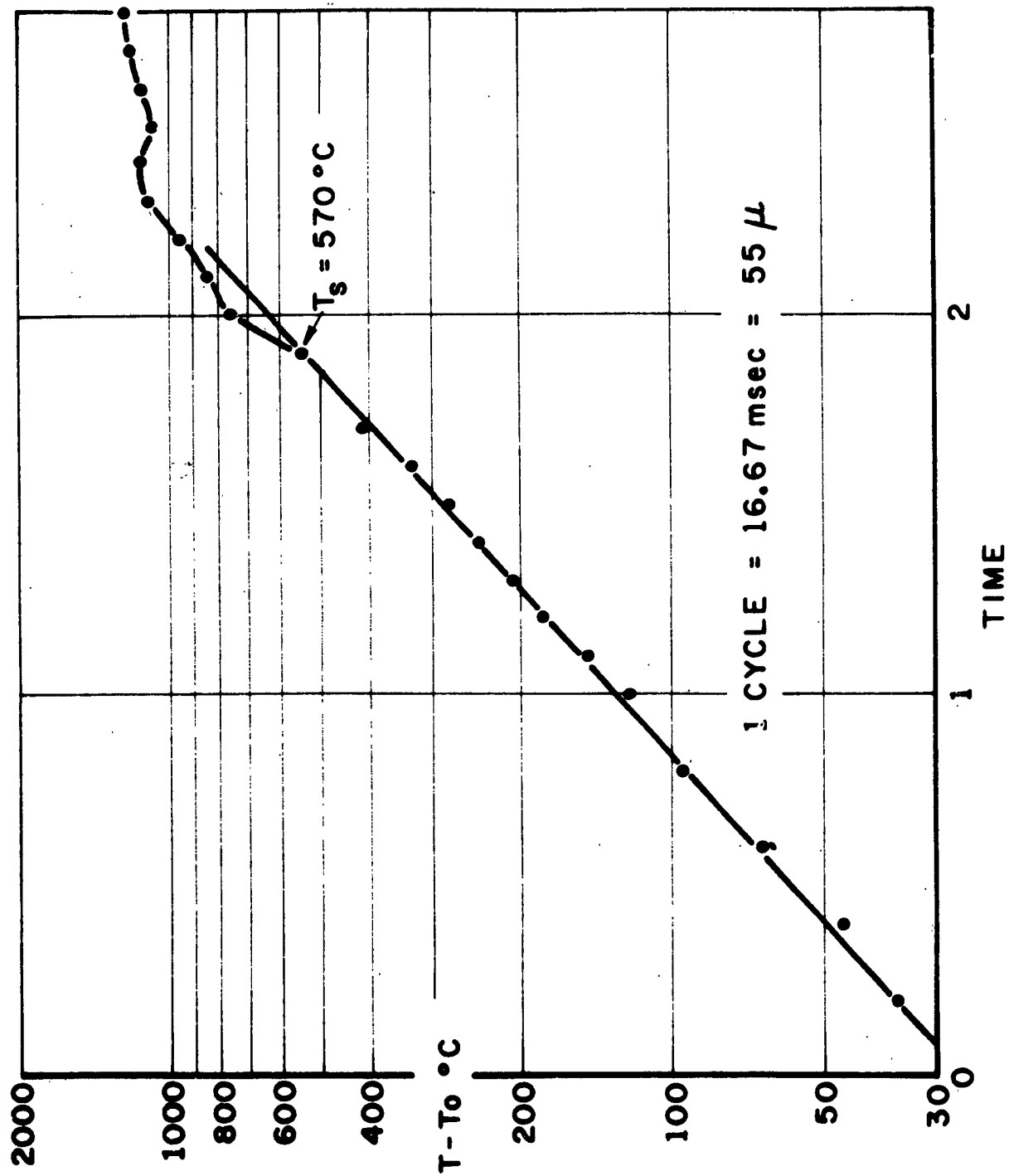
JPR 1957



VOLTAGE - TIME RECORD FOR PBA 70F BURNING AT 30PSIG.
ONE HORIZONTAL DIVISION EQUALS 3.33 mv. DISTANCE BETWEEN
VERTICAL LINES CORRESPONDS TO ONE CYCLE = 16.67 msec.

FIGURE 14A

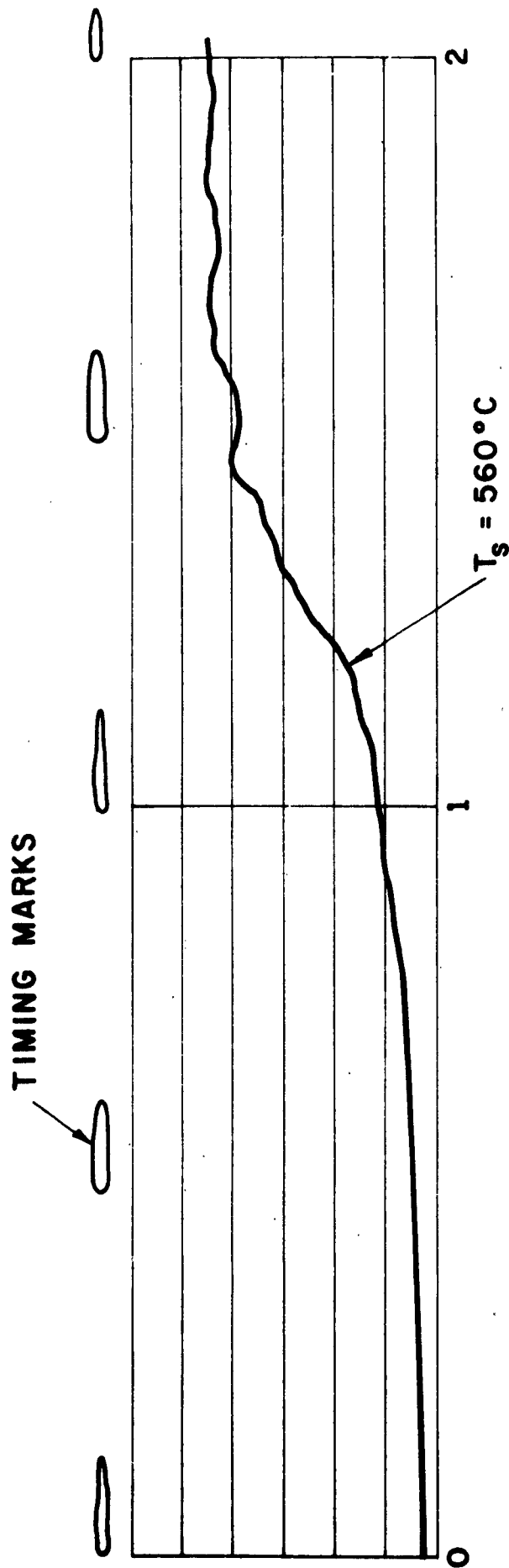
JPR 1981



LOG (T-To) VS TIME CORRESPONDING
TO TEST SHOWN IN FIGURE 14A

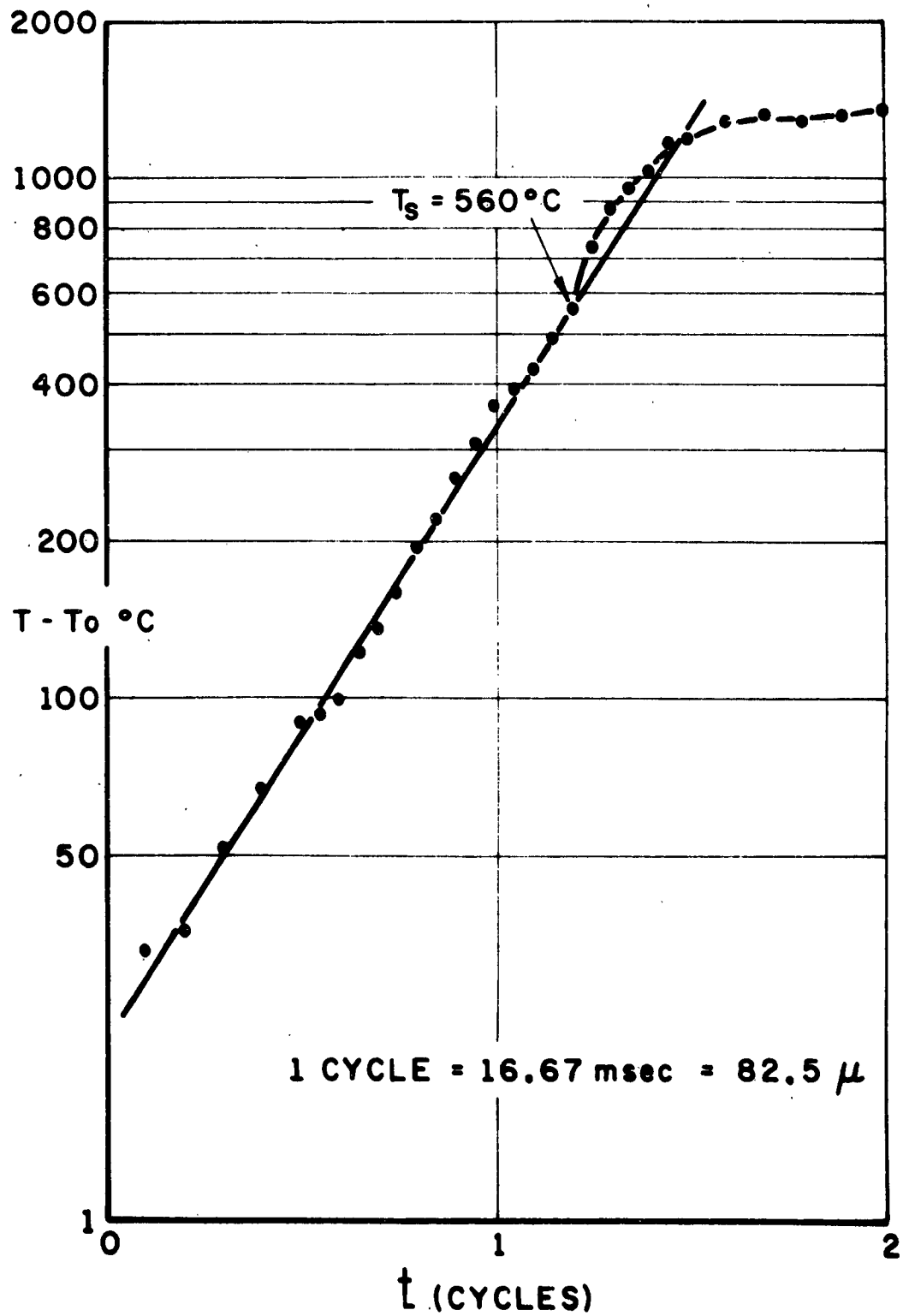
FIGURE 14B

VPR 1988



VOLTAGE - TIME RECORD FOR PBA 70F BURNING AT 100PSIG.
ONE HORIZONTAL DIVISION EQUALS 3.33 mv. DISTANCE
BETWEEN VERTICAL LINES CORRESPONDS TO ONE CYCLE =
16.67 mses.

FIGURE 15A

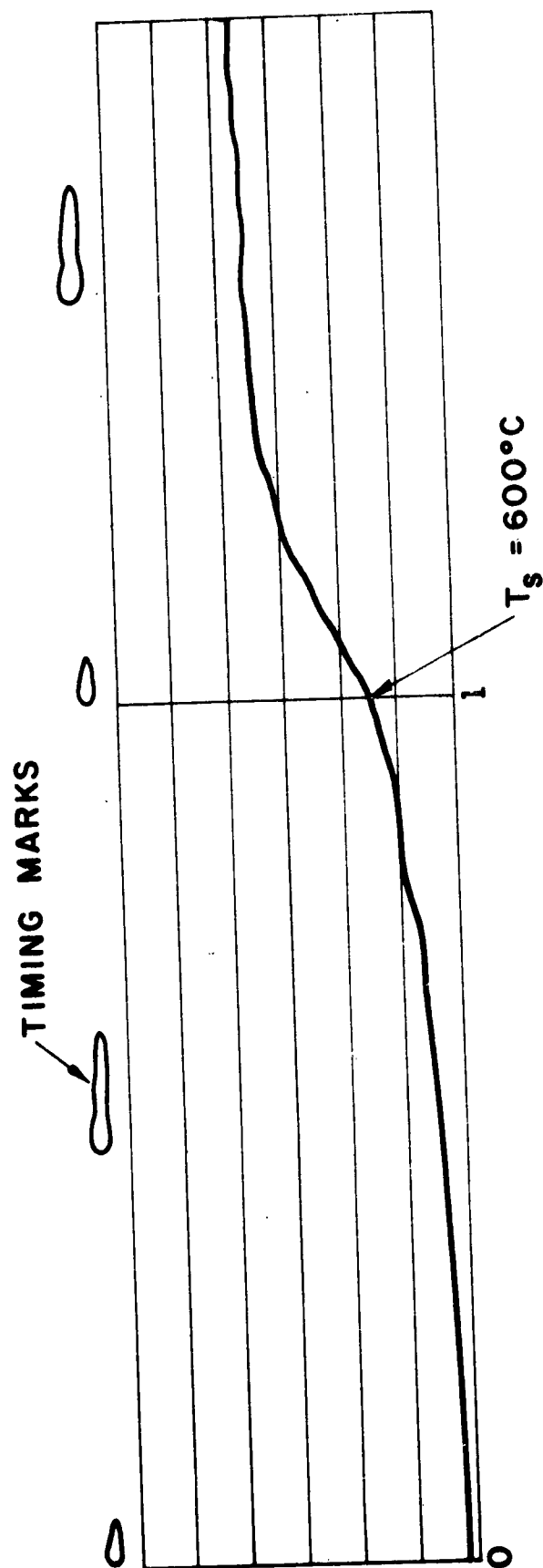


LOG (T-T₀) VS TIME CORRESPONDING
TO TEST SHOWN IN FIGURE 15 A

FIGURE 15B

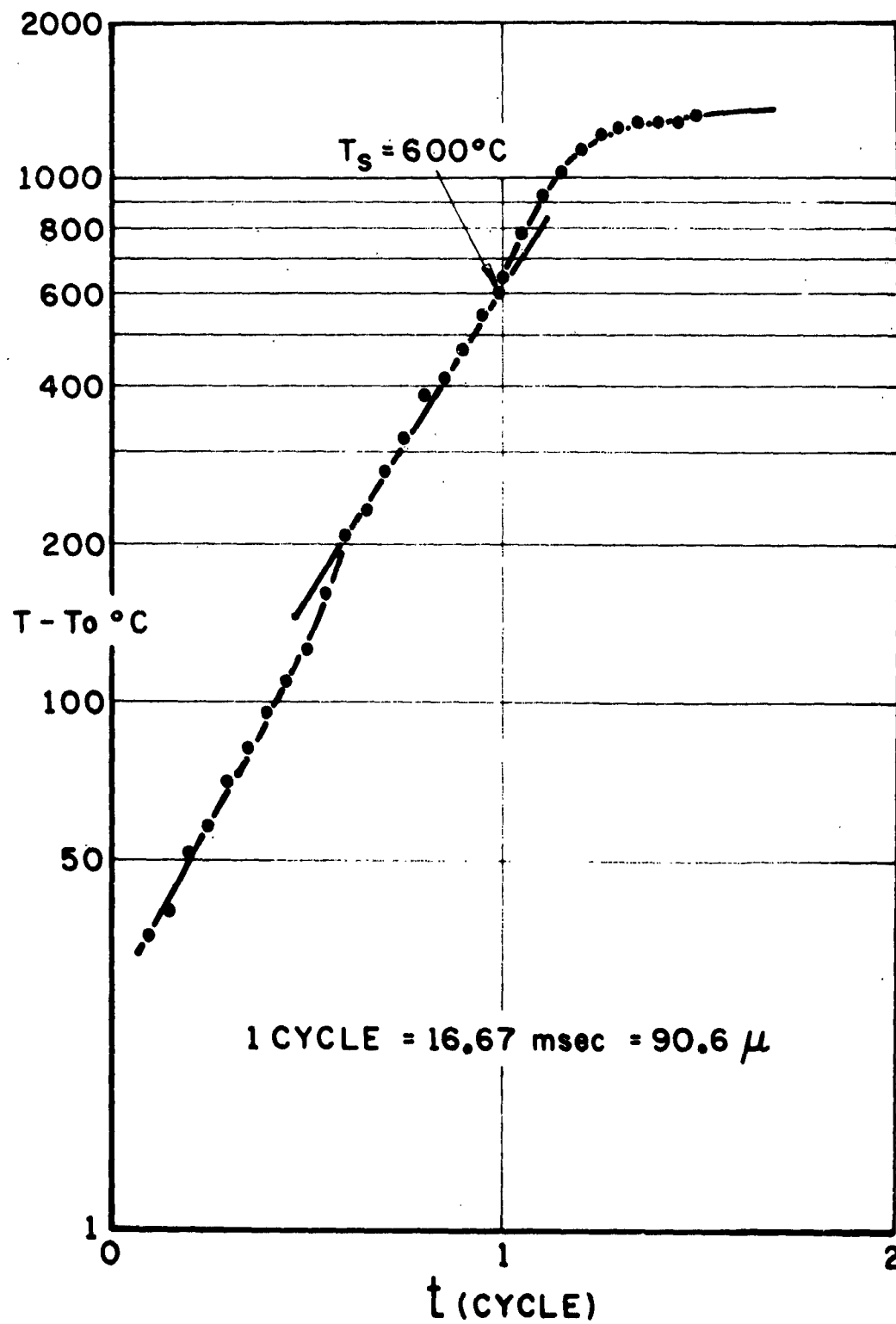
JPL 1950

JPR 1985



VOLTAGE - TIME RECORD FOR PBAA 70F BURNING AT 150 PSIG.
ONE HORIZONTAL DIVISION EQUALS 4mv. DISTANCE
BETWEEN VERTICAL LINES CORRESPONDS TO ONE CYCLE =
16.67 msec.

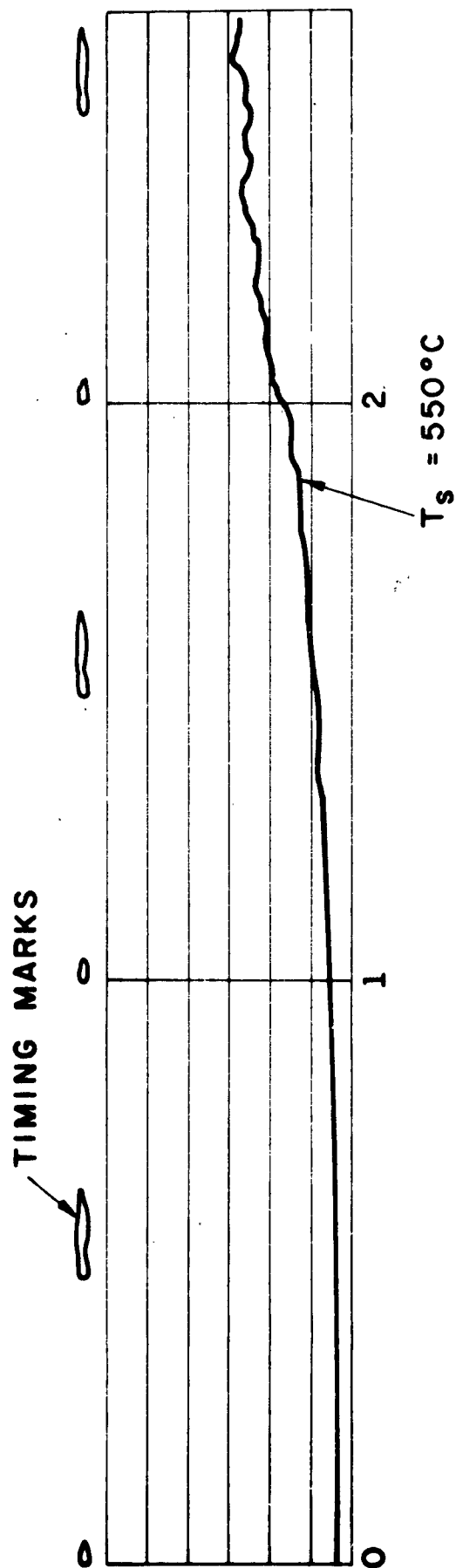
FIGURE 16A



LOG (T-T₀) VS TIME CORRESPONDING
TO TEST SHOWN IN FIGURE 16A

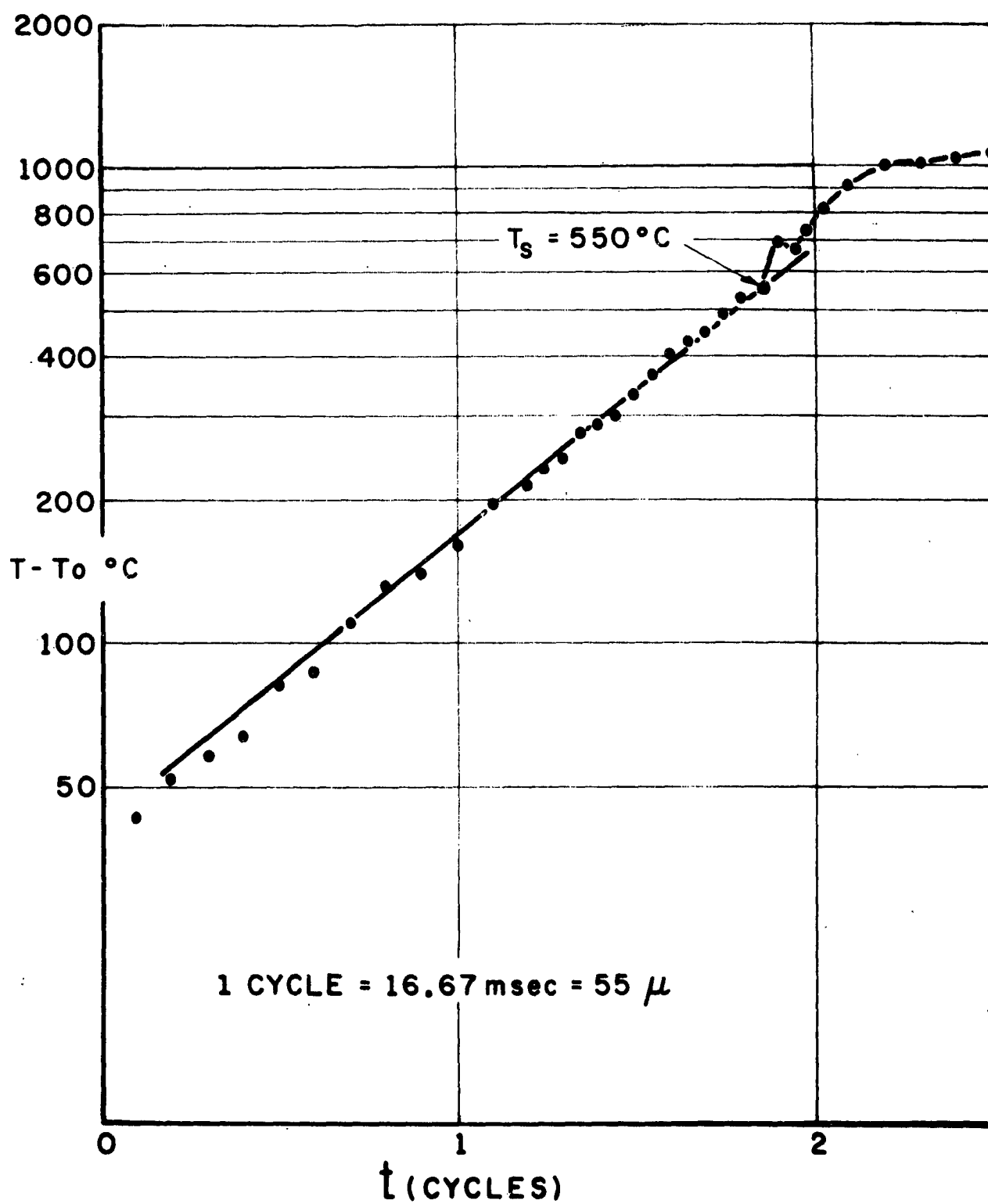
FIGURE 16B

JPR 1934



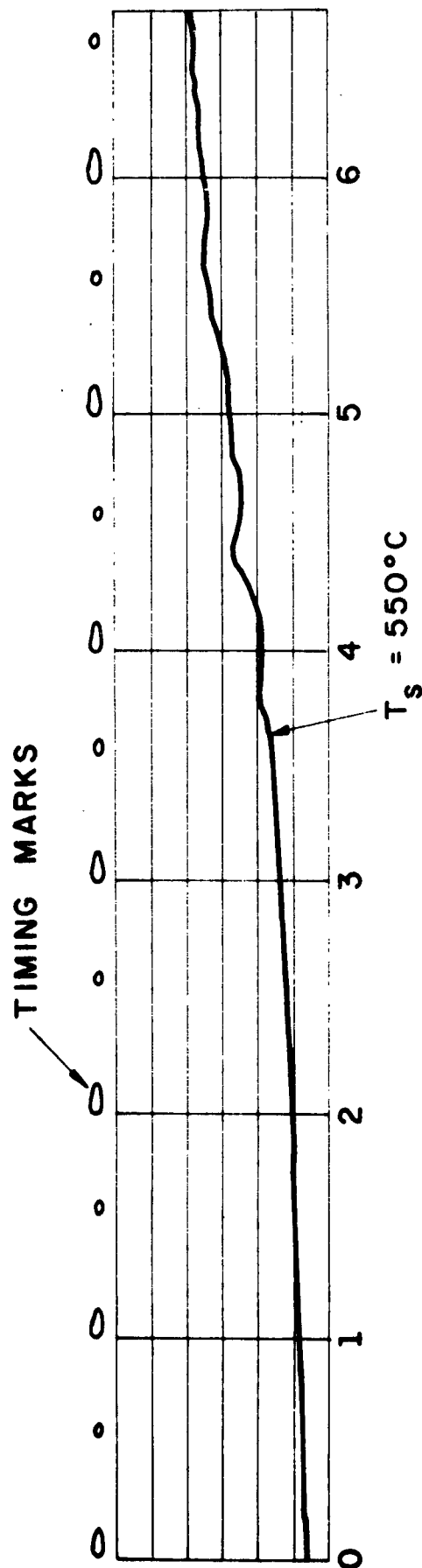
VOLTAGE-TIME RECORD FOR PBAA 70F BURNING AT 30 PSIG.
THERMOCOUPLE OF 2.5μ DIAMETER WIRES. ONE HORIZONTAL
DIVISION EQUALS 5mv. DISTANCE BETWEEN VERTICAL LINES
CORRESPONDS TO ONE CYCLE = 16.67 msec.

FIGURE 17 a



LOG (T-T₀) VS TIME CORRESPONDING
TO TEST SHOWN IN FIGURE 17A

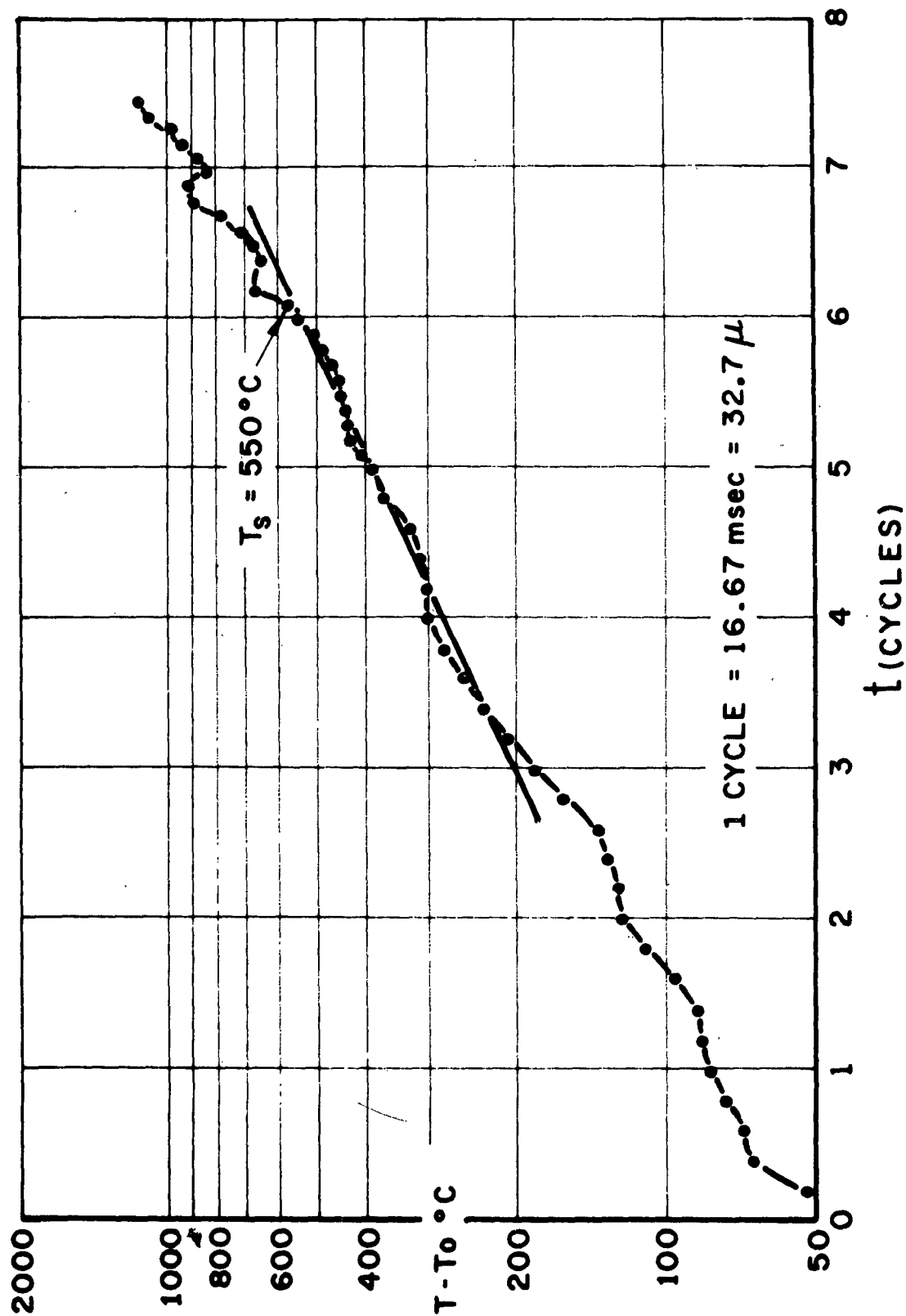
FIGURE 17B



VOLTAGE - TIME RECORD FOR PBAA 75BM BURNING AT
30PSIG. ONE HORIZONTAL DIVISION EQUALS 4mv. DISTANCE
BETWEEN VERTICAL LINES CORRESPONDS TO ONE CYCLE =
16.67 msec.

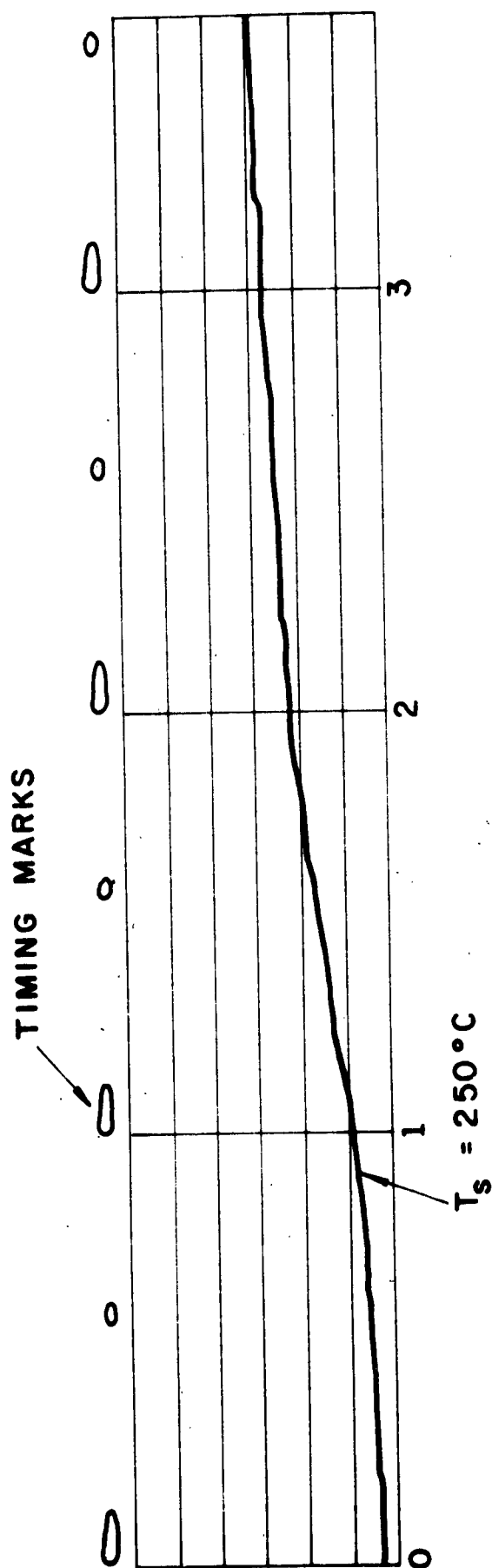
FIGURE 18A

JPR 1977



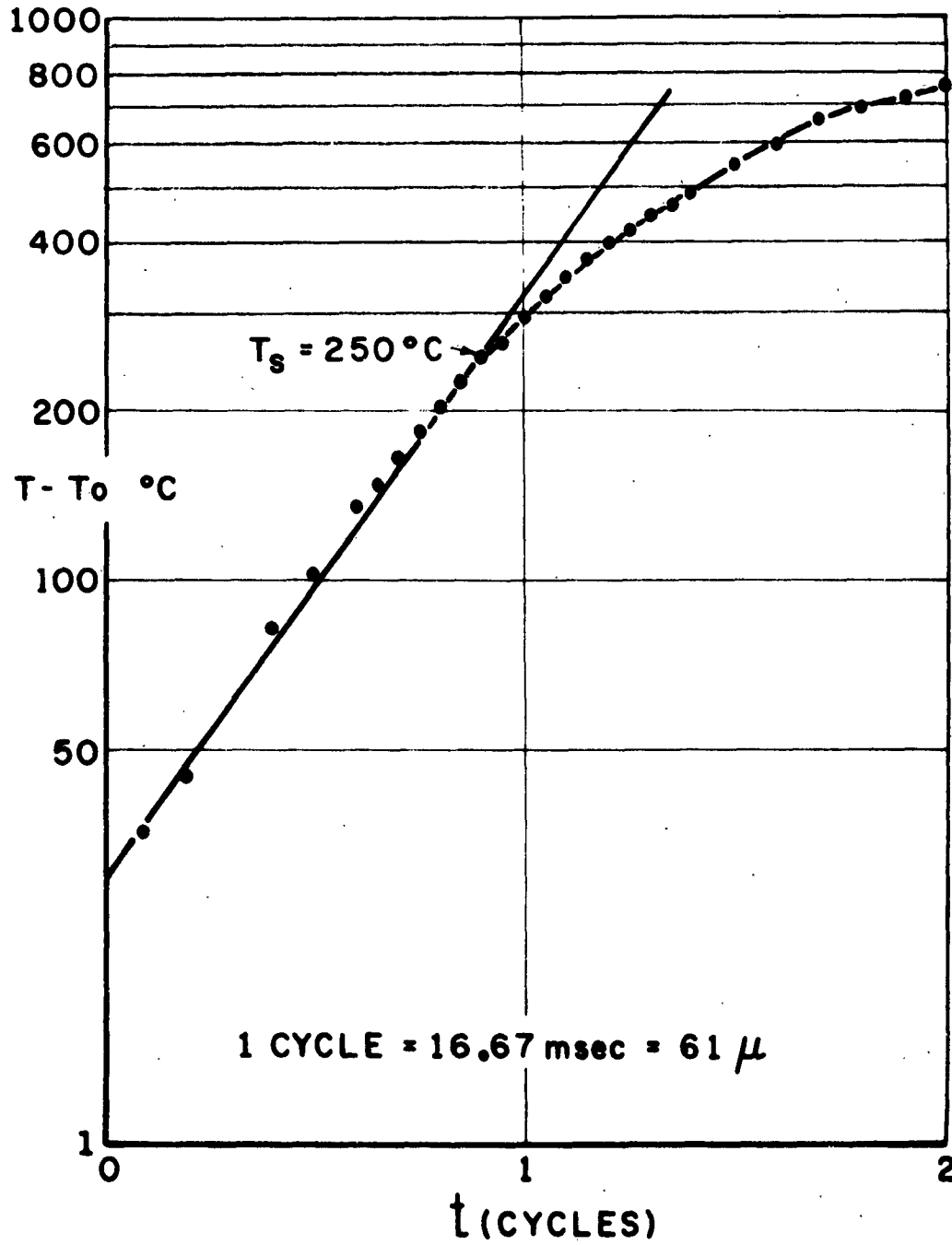
LOG (T-To) VS TIME CORRESPONDING
TO TEST SHOWN IN FIGURE 18A

FIGURE 18 B



VOLTAGE - TIME RECORD FOR DOUBLE-BASE PROPELLANT
 BURNING AT 50 PSIG. ONE HORIZONTAL DIVISION EQUALS
 3.33 mv. DISTANCE BETWEEN VERTICAL LINES CORRESPONDS
 TO ONE CYCLE = 16.67 msec.

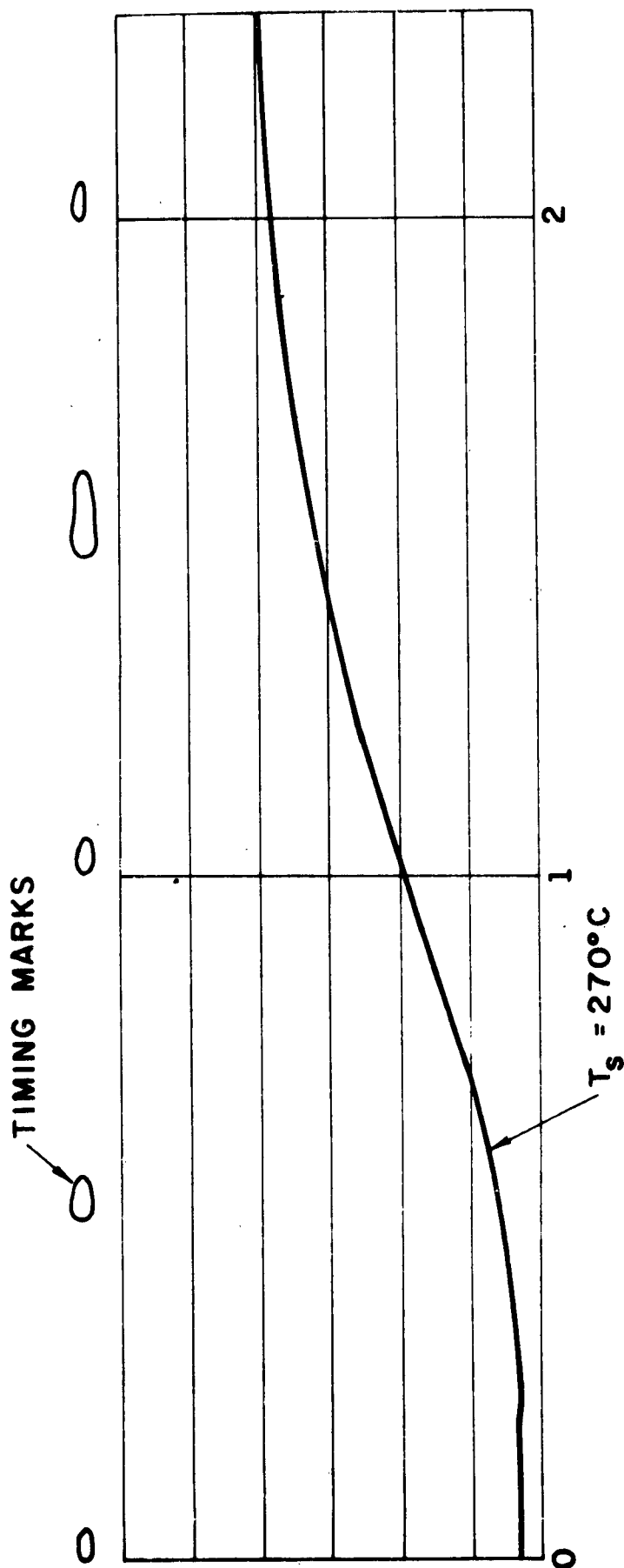
FIGURE 19A



LOG (T-T₀) VS TIME CORRESPONDING
TO TEST SHOWN IN FIGURE 19A

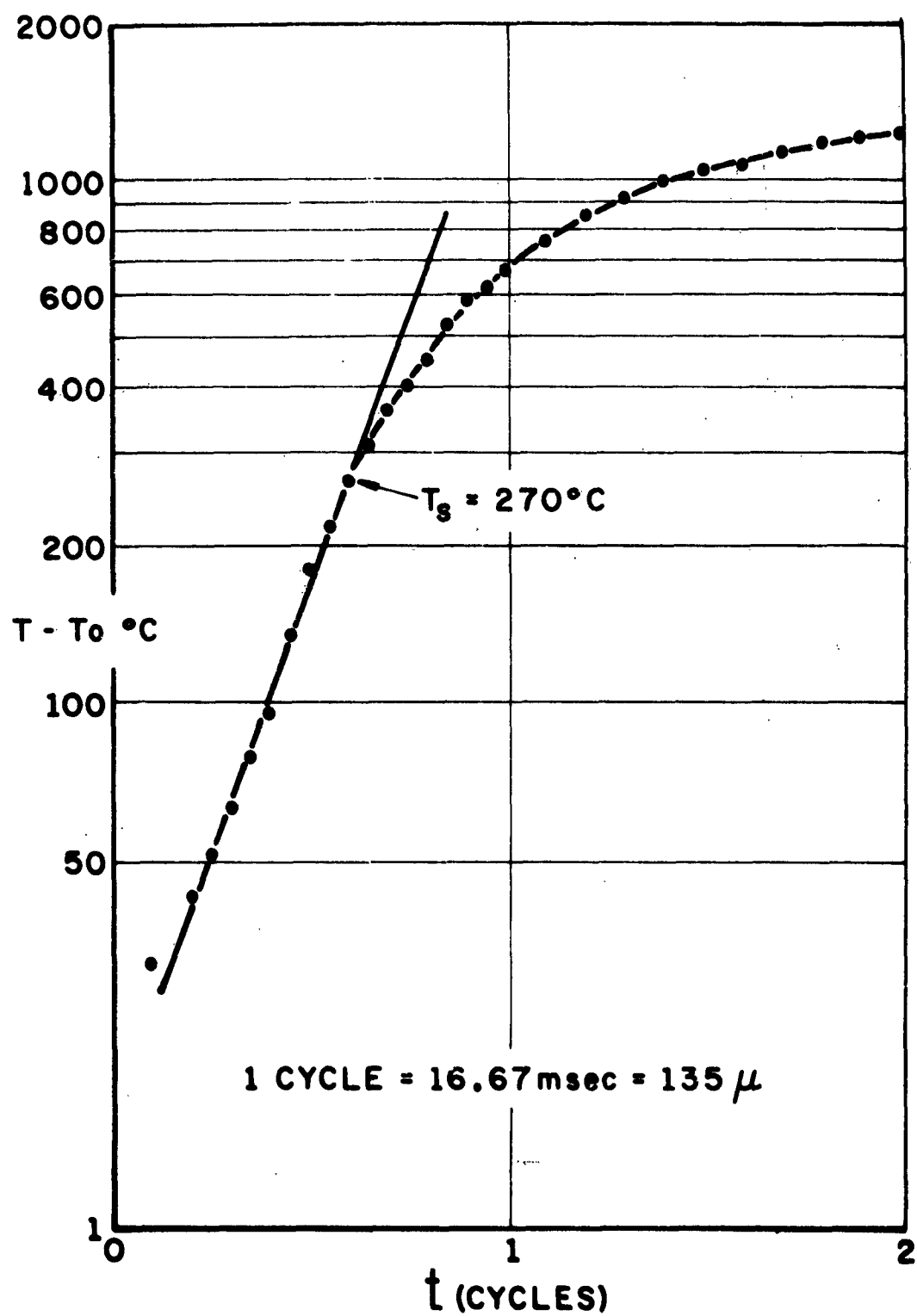
FIGURE 19B

JPR 1986



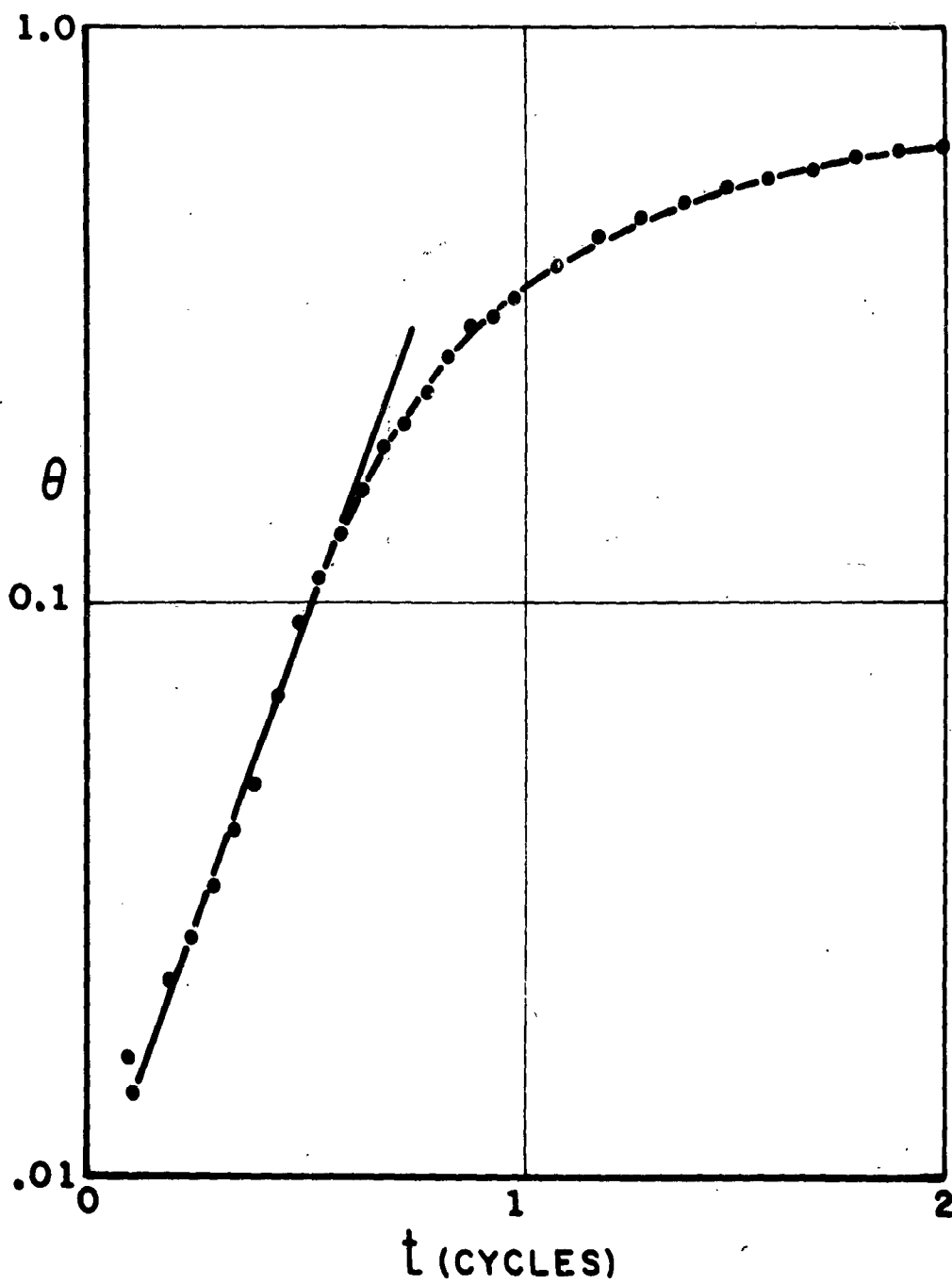
VOLTAGE-TIME RECORD FOR DOUBLE-BASE PROPELLANT
BURNING AT 150 PSIG. ONE HORIZONTAL DIVISION EQUALS
3.33 mv. DISTANCE BETWEEN VERTICAL LINES CORRESPONDS
TO ONE CYCLE = 16.67 msec.

FIGURE 20A



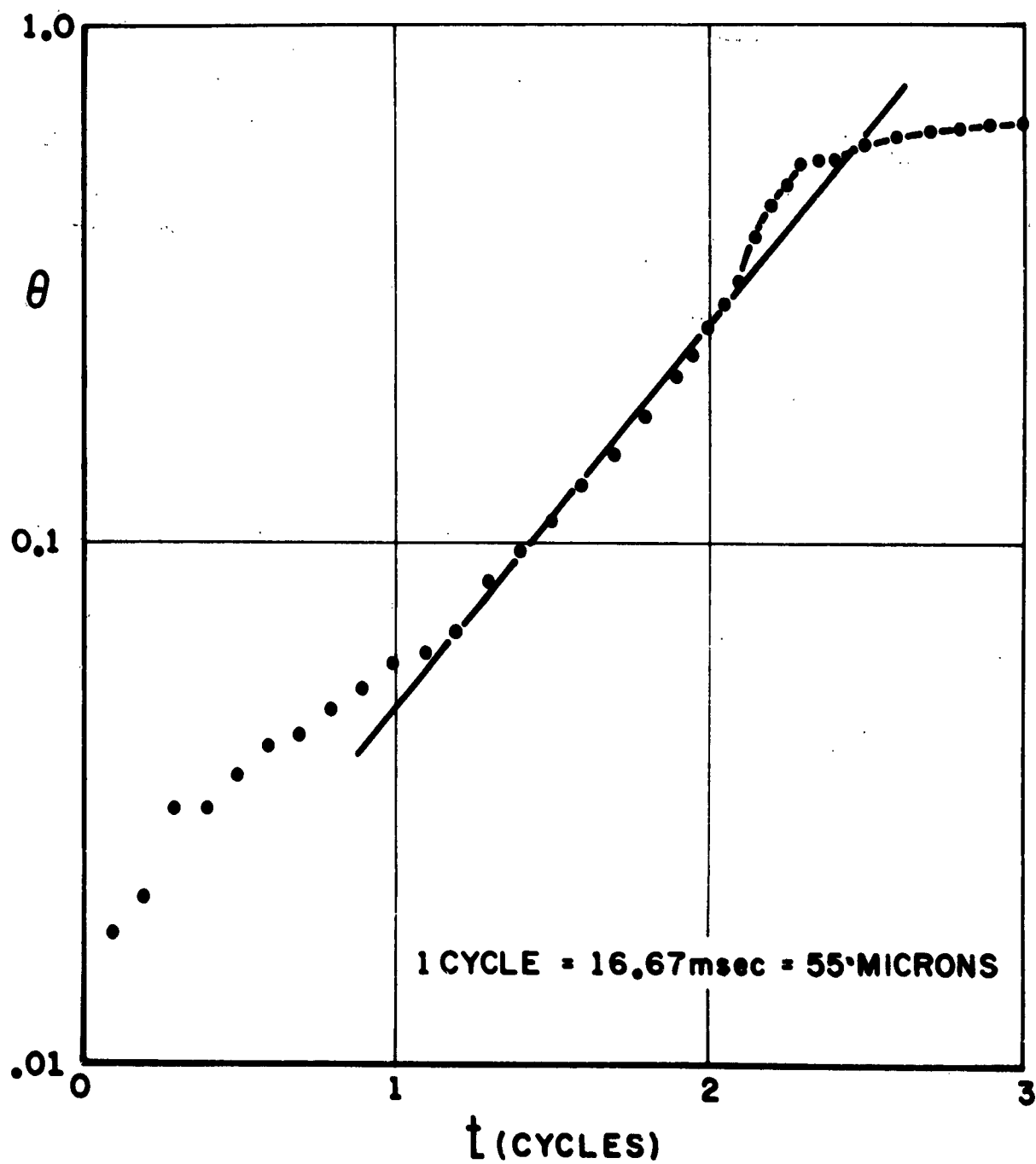
LOG (T-T₀) VS TIME CORRESPONDING
TO TEST SHOWN IN FIGURE 20A

FIGURE 20B



LOG θ VS TIME FOR DOUBLE-BASE PROPELLANT
CORRESPONDING TO TEST SHOWN
IN FIGURE 20A

FIGURE 21



LOG θ VS TIME CORRESPONDING TO
TEST SHOWN IN FIGURE 12

FIGURE 22

JPR 1978

